



Communication for Underwater Sensor Networks: A Comprehensive Summary

AMITANGSHU PAL, Indian Institute of Technology Kanpur, India

FILIPPO CAMPAGNARO, University of Padova, Italy

KHADIJA ASHRAF, MD RASHED RAHMAN, and ASHWIN ASHOK,

Georgia State University, USA

HONGZHI GUO, Norfolk State University, USA

Sensing and communication technology has been used successfully in various event monitoring applications over the last two decades, especially in places where long-term manual monitoring is infeasible. However, the major applicability of this technology was mostly limited to terrestrial environments. On the other hand, **underwater wireless sensor networks (UWSNs)** opens a new space for the remote monitoring of underwater species and faunas, along with communicating with underwater vehicles, submarines, and so on. However, as opposed to terrestrial radio communication, underwater environment brings new challenges for reliable communication due to the high conductivity of the aqueous medium which leads to major signal absorption. In this paper, we provide a detailed technical overview of different underwater communication technologies, namely acoustic, magnetic, and visual light, along with their potentials and challenges in submarine environments. Detailed comparison among these technologies have also been laid out along with their pros and cons using real experimental results.

CCS Concepts: • **Hardware** → **Sensor applications and deployments; Sensor devices and platforms; Networks** → **Sensor networks**;

Additional Key Words and Phrases: Underwater communication, channel modeling, RF communications, acoustic communications, magnetic induction communications, visual light communication

ACM Reference format:

Amitangshu Pal, Filippo Campagnaro, Khadija Ashraf, MD Rashed Rahman, Ashwin Ashok, and Hongzhi Guo. 2022. Communication for Underwater Sensor Networks: A Comprehensive Summary. *ACM Trans. Sensor Netw.* 19, 1, Article 22 (December 2022), 45 pages.

<https://doi.org/10.1145/3546827>

Hongzhi Guo was supported by The Thomas F. and Kate Miller Jeffress Memorial Trust, Bank of America, Trustee. The work performed by Filippo Campagnaro has been partially supported by the European Union - FSE REACT EU, PON Research and Innovation 2014-2020 (DM 1062/2021).

Authors' addresses: A. Pal (corresponding author), Indian Institute of Technology Kanpur, Kanpur, Uttar Pradesh, 208016, India; email: amitangshu@cse.iitk.ac.in; F. Campagnaro, University of Padova, Padova, Veneto, 35131, Italy; email: campagn1@dei.unipd.it; K. Ashraf, MD R. Rahman, and A. Ashok, Georgia State University, 25 Park Place, Atlanta, Georgia, 30303, USA; emails: {[kashraf1](mailto:kashraf1@student.gsu.edu), [mrahman19](mailto:mrahman19@student.gsu.edu)}@student.gsu.edu, aashok@gsu.edu; H. Guo, Norfolk State University, 700 Park Ave, Norfolk, VA, 23504, USA; email: hguo@nsu.edu.

Permission to make digital or hard copies of all or part of this work for personal or classroom use is granted without fee provided that copies are not made or distributed for profit or commercial advantage and that copies bear this notice and the full citation on the first page. Copyrights for components of this work owned by others than ACM must be honored. Abstracting with credit is permitted. To copy otherwise, or republish, to post on servers or to redistribute to lists, requires prior specific permission and/or a fee. Request permissions from permissions@acm.org.

© 2022 Association for Computing Machinery.

1550-4859/2022/12-ART22 \$15.00

<https://doi.org/10.1145/3546827>

1 INTRODUCTION

The applications of **wireless sensor networks (WSNs)** are not only limited to terrestrial applications, but also have huge potential in various underwater monitoring applications like marine habitat monitoring, underwater disaster monitoring, oil/gas pipeline monitoring, and so on. Such applications require continuous, non-intrusive communication mechanisms that work well in underwater environments. However, **underwater wireless sensor networks (UWSNs)** bring a number of challenges that are unique as compared to the terrestrial environments, mainly due to the conductivity of the water medium which also increases with the salinity level. **Radio frequency (RF)** based communications are extensively studied in terrestrial applications, however, the **electromagnetic (EM)** wave is absorbed in water medium, and thus cannot work well in deep marine environments. Reducing signal absorption can be achieved by using lower frequencies, but this severely limits the achievable data rate and requires bigger antennas.

Acoustic communication is another promising communication technology and works well in aqueous media. However, the low propagation speed of sound (i.e., 1500 m/s) results in long message delays for acoustic communication. In addition to that, multi-path fading and Doppler effects of acoustic signals also limit the communication quality [1]. Due to this long delay and multi-path effects, such communication is also affected by underwater turbulence and suspended sediments [2]. In addition to these, the communication is adversely affected due to the multiple reflected paths at the water-air boundary [3, 4], which limits the communication quality especially in shallow water.

Visible light communication (VLC) is another emerging technology that is standardized by IEEE in 2011 in the form of IEEE 802.15.7. The technology can achieve 100 Mb/sec or higher transmission rate for line-of-sight communications. VLC also experiences low signal attenuation in water and has already shown promise in achieving high-speed underwater communication spanning up to hundreds of meters (≈ 300 m) [5]. The light absorption is minimum at 400–500 nm of the visible spectrum, however, the characteristics change based on the amount of phyto-plankton species and dissolved underwater organic matters. **Underwater wireless optical communication (UWOC)** is also impacted by underwater scattering due to density fluctuations, organic and inorganic large particles. The communication also deteriorates in the presence of underwater obstacles such as marine species.

Another emerging and popular technology for underwater communication is **Magnetic Induction (MI)** based communication that works on the principle of resonant inductive coupling, where two matched LC coils communicate with the same resonance frequency. MI communication has higher propagation speed (3×10^8 m/s) as compared to acoustic communication. In addition to that, the communication is purely magnetic, and therefore does not suffer from multi-path fading and diffraction effects. Because of negligible multi-path effects, MI communication is less affected by turbulence and less impaired in shallow water [4]. The communication quality is also not disturbed in the water/air boundaries, because of similar magnetic permeabilities of these media. However, MI signal strength drops very fast, and therefore the transmission range is relatively limited.

In this paper we provide a detailed overview of different communication technologies in underwater environments, along with their potentials, challenges and applicability. As the topic is quite broad in nature, there are few survey articles [6, 7] that are studied in the literature on this topic. In particular, the survey in [8] focuses on underwater magnetic induction communication, the survey in [9] focuses on underwater optical communication, and the survey in [10] focuses on underwater acoustic communication systems. However, as opposed to these literature, we provide a detailed comparison of these different technologies considering experimental prototyping, which are sparse in the other surveys. We also discuss relevant challenges corresponding to different wireless technologies.

The paper is structured as follows. Section 2 discusses several application scenarios for underwater communication. Sections 3–6 extensively summarize several research studies and limitations of RF, acoustic, VLC, and MI communication for UWSNs. Comparison of different technologies along with relevant discussions are summarized in Section 7. The paper is concluded in Section 8.

2 DIFFERENT USE CASES OF UNDERWATER COMMUNICATION

The applications of **underwater WSNs (UWSNs)** have huge potential for monitoring the health of marine aquaculture, underwater pollution detection and control, underwater habitat monitoring, climate monitoring and tracking any disturbances, and so on. Below we discuss some of the major applications of UWSNs.

Underwater Marine Life Monitoring: Marine habitat monitoring was one of the main application areas of underwater wireless sensor networks. One of the prominent applications is monitoring fishing activities. Fisheries are an important source of income for a large number of people worldwide; however, poorly managed capture of fish will disturb the marine ecosystems. Therefore, a sustainable fisheries management requires a careful management of the amount and effect of fishing, which can be achieved by remotely monitoring the seabed habitats using sensing technology such as remote cameras [11]. These cameras can be attached with **Autonomous underwater vehicles (AUVs)** that can gather imagery data, which can be analyzed for undersea habitat monitoring [12, 13].

Many other similar exercises have been conducted for monitoring the marine habitats. ACME [14] is a European funded project designed for permanent monitoring of marine activities, especially in areas like shipping lanes, estuaries, and the like [15]. Similar other projects are LOTUS [16] and SWAN [17]. CoralSense [18] and SEA-LABS [19] have studied the use of UWSN for coral reef habitat monitoring. Authors in [20] have investigated the potential of high-frequency multibeam sonar as a means of remotely collecting high-resolution movement data for marine mammals. In [21] the authors have developed an underwater video system called *PelagiCam* for semi-automated monitoring of mobile marine fauna.

Underwater Resource Monitoring: UWSN are also useful for exploring various underwater natural resources like oil/gas extraction, oil spills, mine detection, and so on. According to a report [22, 23], the global underwater monitoring of oil and gas market is expected to surpass 1.8 billion dollars by 2024. At the same time, increasing numbers of accidents at the drilling facilities also boost the need for a large-scale underwater monitoring system. In [24] the authors have used acoustic communication along its visual mapping to monitor underwater manganese crust. Other studies on deep sea exploration are also reported in [25]. In addition, the increasing applications and researches of underwater robotics and unmanned autonomous vehicles [26] are also aiding the need for such underwater monitoring where communication in the underwater medium is a vital requirement.

Monitoring Underwater Pipelines: Underwater pipeline infrastructures are typically used for transferring water, petroleum, and natural gas. These pipelines span over large areas; for example, the Langede pipeline [27] that transfers natural gas to England extends over 1,200 km from the Ormen Lange field in Norway to the Easington Gas Terminal in England. This pipeline carries around 25.5 billion cubic meters of natural gas per year. Another long pipeline of 364 km is located between Qatar and UAE under the Arabian Gulf, that is used to transfer processed natural gas [28]. Apart from these, there are around 30,000 miles of underwater pipelines in the Gulf of Mexico to transfer oil [29].

However, over time such long pipelines experience leakage, corrosion, dents, and cracks. Contamination goes hand in hand with leakage due to seepage through leaks, rusted pipes, and internal build ups. Cracks in pipelines carrying oil and gasses can be quite fatal and may lead to

environmental pollution. For example, in 2010 a ruptured pipeline spewing natural gas caused a blast in San Bruno, California, that left behind a 72 foot long crater, killed eight people, and injured more than fifty [30]. Another pipeline accident took place near Michigan, which led to the spilling of 840,000 gallons of crude oil into the Kalamazoo River with an estimated cost of 800 million dollars [30]. To avoid such incidents, a continuous monitoring of these pipeline infrastructures through the deployment of sensor nodes across the pipelines are crucial. Several studies for underwater cable and pipeline monitoring applications that are deployed for oil or gas extraction are reported in [31–33].

Underwater Disaster Monitoring: UWSN is also useful for monitoring underwater disasters such as underwater volcanic eruptions, underwater earthquakes that result in tsunamis, and floods. After the 2004 tsunami that caused extensive damage and deaths in Indonesia, scientists have expanded the ocean-based warning system called **DART (Deep-ocean Assessment and Reporting of Tsunamis)** in the Indonesian archipelago [34]. The system consists of pressure sensors that are deployed at the seafloor to relay signals to the shore, which can be used to estimate the possibility of potential tsunamis. UWSNs can also be used for developing underwater seismic monitoring stations. A team of marine scientists from **Woods Hole Oceanographic Institution (WHOI)** are using radio telemetry to monitor the rumblings of a submarine volcano (named Kick'em Jenny, which is an active volcano under Caribbean Sea) from seismic monitoring devices installed on the volcano [35]. The seismic data from these devices are transmitted from a high-frequency radio to a land-based observatory, which helps the scientists to observe the state of the volcano as it draws in and expels seawater, magma, and super-heated fluids.

Underwater communication has also been used to locate the underwater wreckage and debris after any accidental crash during investigation and searching. For example, underwater AUVs were deployed in the aftermath of AirFrance Flight 447 crash in the Atlantic Ocean in 2010. Three REMUS 6000 AUVs were deployed to search for the plane wreckage; each one of them searched an area of approximately 40.6 square kilometers by day [36]. Finally in 2011, the plane wreckage was detected and confirmed by the side scan sonar and the AUV cameras. These applications require communicating the monitoring data to an above-ground monitoring station, thus, underwater communication is essential in such scenarios.

Monitoring Underwater Climate Change: UWSN also has the potential to monitor climate change under the ocean surfaces. For example, the Argo program (<https://argo.ucsd.edu/>) was initiated with the key objective of monitoring the ocean data related to climate change. The project uses robotic instruments that drift with the ocean currents and move up and down between the surface and a mid-water level [37]. These instruments measure temperature and salinity of the water, along with other properties related to the biology/chemistry of the ocean. In 2020, Argo has collected 12,000 data profiles each month; these measurements provide crucial information, such as ocean heat content increases and sea level rises, and the like, to the scientists. For example, temperature measurements obtained from the sensors allow the researchers to monitor the spatio-temporal distribution of heat changes over the years.

Based on the requirement of the use cases, the above mentioned application scenarios can be divided into two categories: continuous communication or monitoring, and event-driven monitoring, as shown in Figure 1. For example, monitoring applications like marine life, underwater resources, and climate requires transmitting the sensed data continuously; therefore the primary **Quality of Service (QoS)** requirement for these applications is the low energy consumption of the sensing devices. On the other hand, underwater pipeline monitoring (for leaks, contamination, etc.) or disaster monitoring does not require the sensing nodes to send data continuously, but whenever such events are detected, they need to be reported with high reliability and with low latency. In the following sections, we study different wireless communication technologies

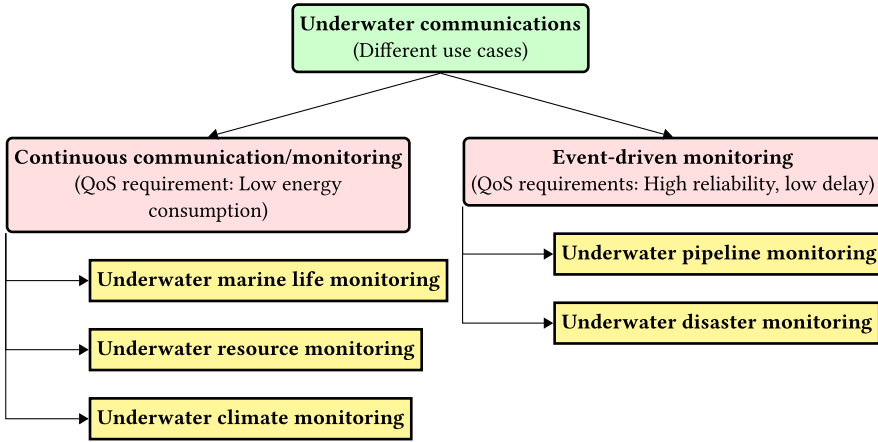


Fig. 1. Taxonomy of different use cases for underwater communications.

(i.e. RF, optical, acoustics, and magnetic) along with their possibilities and limitations for various underwater applications.

3 DISCUSSION OF RF TECHNOLOGIES AND THEIR LIMITATIONS

Radio Frequency (RF) based communications have been studied and researched ubiquitously both for long range and short range communications. Underwater RF communication has been investigated during the early days of radios [38]. However, RF propagation through water is quite different than that of through air; the channel attenuation factor α in water can be represented as [39]

$$\alpha = \sqrt{\pi \sigma \mu_0 f} \quad (1)$$

where σ is the water conductivity (in Siemens/meter), f is the frequency (in Hertz) and μ_0 is the permeability (in henry/meter). Due to high electrical conductivity, underwater channel experiences strong signal attenuation. Therefore, the underwater media causes high signal absorption and diffraction and results in an extremely complex and lossy communications channel. From Equation (1) we can also observe that the attenuation is proportional to the water conductivity, which depends on the level of salinity. The conductivity of sea water is 4.3 S/m, whereas that of fresh water is 0.001 to 0.01 S/m. Therefore, the attenuation of RF signal is higher in sea water than in fresh water. In [2] the authors have studied RF skin depth, propagation velocity, and path loss at different frequencies in underwater medium. Other theoretical modeling of propagation characteristics in underwater scenarios are reported in [40, 41].

Table 1 shows channel characteristics of different RF bands in underwater medium, where e-folding depth is the depth at which the signal's intensity is reduced from its surface intensity by a factor of $1/e$ (where $e = 2.72$) [42]. As the attenuation increases with frequency, establishing a reliable communication link underwater is quite difficult in **very and ultra high frequency (VHF and UHF)** range; in fact in HF and MF range also the e-folding depth is quite small. Therefore, the studies for underwater RF communication in this range is quite limited. In [43] the authors have studied underwater communication in 2 MHz, 50 MHz, and 2.4 GHz bands. Underwater RF communication in 2.4 GHz is reported in [44, 45]. However, these studies have been conducted in low depth and so are not applicable for general UWSN applications.

Table 1. Characteristics of Different RF Frequency Bands for UWSNs [42]

Frequency band	Frequency range (Hz)	Wavelength range (m)	e-folding depth (m)
Extremely High Frequency (EHF)	$3 \times 10^{10} - 3 \times 10^{11}$	$10^{-2} - 10^{-3}$	-
Super high Frequency (SHF)	$3 \times 10^9 - 3 \times 10^{10}$	$10^{-1} - 10^{-2}$	-
Ultra High Frequency (UHF)	$3 \times 10^8 - 3 \times 10^9$	$1 - 10^{-1}$	-
Very High Frequency (VHF)	$3 \times 10^7 - 3 \times 10^8$	$10 - 1$	-
High Frequency (HF)	$3 \times 10^6 - 3 \times 10^7$	$10^2 - 10$	0.14 - 0.05
Medium Frequency (MF)	$3 \times 10^5 - 3 \times 10^6$	$10^3 - 10^2$	0.46 - 0.14
Low Frequency (LF)	$3 \times 10^4 - 3 \times 10^5$	$10^4 - 10^3$	1.4 - 0.46
Very Low Frequency (VLF)	$3 \times 10^3 - 3 \times 10^4$	$10^5 - 10^4$	4.6 - 1.4
Extremely Low Frequency (ELF)	$3 - 3 \times 10^3$	$10^8 - 10^5$	144 - 4.6

On the other hand, reducing absorption by choosing lower frequencies helps in attenuation [46, 47]; in fact, **extremely low frequency (ELF)** submarine communication was studied for sub-sea electromagnetic application [48, 49]. The system used to operate at 76 Hz for the US system and 82 Hz for the Russian system with an extremely low data rate of few characters per minute [38]. In [50] the authors have studied the RF path loss from air to water in between 23 kHz to 1 GHz. They have identified an optimal frequency range of 3-100 MHz when the wave propagates to depths less than 5 meters; however, the loss increases monotonically when the depth is more than 10 meters. Similar studies for underwater communication vehicles are studied in [51–54].

However, using low frequencies for RF communication needs bigger antennas, which introduces the problem on undesirable size and potentially severe interference with nearby radios. Also as the underwater RF communication is limited to very low frequency, the available bandwidth is quite small, which severely limits the data rate. VLF only offers a few hundred bps, whereas ELF supports only a few bits per minute [55], which prevents transmission of complex data. Because of these issues, a long range and high data rate RF communication through water is found to be impractical for many real-world applications. Therefore, below we study the other three means of communications (i.e. acoustic, optical, and magnetic) in greater details.

4 ACOUSTIC BASED UNDERWATER COMMUNICATIONS

Another technology of interest for challenging environments is acoustic communications which is based on the propagation of high frequency pressure waves through the media. Acoustic propagation is heavily studied in underwater environments where it can be used for very low-data rate (at most a few kb/sec) communications over a few kilometers [56–59].

This section is organized as follows. We first discuss relevant acoustic communication characteristics (i.e. propagation loss, delay, signal-to-noise ratio, etc.) in underwater medium in Sections 4.1–4.3. Common acoustic modems are discussed in Section 4.4. We then report some measurement studies on acoustic communication in Section 4.5. Practical issues and future research challenges are then reported in Sections 4.6–4.7.

4.1 Underwater Acoustic Propagation Loss

The underwater acoustic transmission range strongly depends not only on the transmission power, but also on the frequency and the bandwidth of the signal. Specifically, the attenuation experienced by a signal with carrier frequency f at distance d and expressed in dB, can be computed as [60]:

$$A(d, f)_{dB} = k \cdot 10 \log d + d \cdot a(f), \quad (2)$$

where k is the spreading factor, used to describe the geometry of the propagation, and $a(f)$ is the absorption loss.

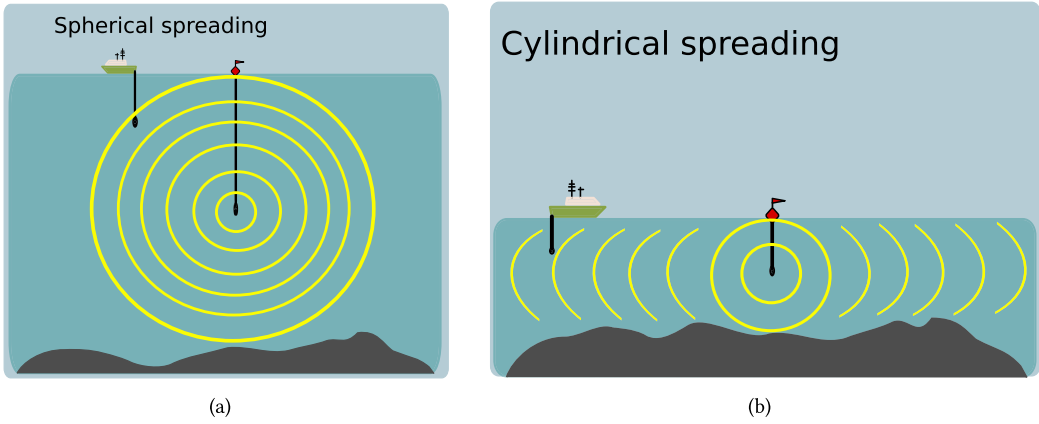


Fig. 2. Spherical spreading is (a) experienced when a sound wave propagates away from a source uniformly in all directions, and cylindrical spreading is (b) experienced when the acoustic signal systematically propagates in a medium with upper and lower boundaries.

With $k = 2$ we have the so called spherical spreading (Figure 2(a)), experienced when a sound wave propagates away from a source uniformly in all directions, such as when an acoustic source is placed at mid-depth of the water column in a deep water scenario, and the distance d between transmitted and receiver is less than (a) the distance between the transmitter and the sea bottom, and (b) the distance between the transmitter and the sea surface. With $k = 1$, instead, we have the cylindrical spreading (Figure 2(b)), experienced when the acoustic signal systematically hits the sea surface and the sea floor before reaching the destination, thus propagates in a medium with upper and lower boundaries. A cylindrical spreading assumes that the sound is distributed uniformly over the surface of a cylinder having the radius equal to the transmission range d and the height equal to the depth of the ocean. The propagation can be approximated as cylindrical whenever d is way greater than the water depth (e.g., at least two times the water depth). In this case the acoustic signal attenuates slowly than in the case of spherical spreading, but is more affected by self interference due to reflections with the sea floor and the sea surface.

Finally, with $k = 1.5$ we can approximate the case when d is larger than half of the water depth, but not large enough to entail a cylindrical spreading. This is the most common case experienced in the field, and for this reason $k = 1.5$ is called practical spreading.

The absorption loss $a(f)$ is usually expressed empirically, by using the formula that best approximates the absorption of a certain acoustic frequency in a determinate area. For instance, the Thiele’s formula [61] is proved to well represent the propagation loss in the cold shallow waters of the Baltic and the North Sea, while the model proposed by Chitre in [62] best describes the acoustic propagation in the warm Singapore waters. The Thorp’s formula [63], however, is still the most commonly used to compute the path-loss, and is presented as follows:

$$10 \log a(f) = \frac{0.11 \cdot f^2}{1 + f^2} + \frac{44 \cdot f^2}{4100 + f^2} + 2.75 \cdot 10^{-4} f^2 + 0.003, \tag{3}$$

with f expressed in kHz. This formula provides the absorption coefficient in dB/km of a single propagation path: this coefficient increases rapidly with frequency, hence imposing a limit on the maximum frequency that can be used for an acoustic transmission at a given distance.

While a single propagation path model can be used to model an acoustic transmission in a vertical channel, where the signal reflections with the sea bottom and the sea surface can be neglected,

it cannot be used to model horizontal transmissions, where the multipath effect caused by the signal reflections plays an important role. In this case models that well characterize the secondary paths need to be used. Among the existing models [64, 65], the most commonly used is the Bellhop ray tracer [66], that, given the environmental conditions of a certain area, provides as results an accurate model for the sound propagation. Specifically, the parameters considered to characterize the environmental conditions of a certain area are: bathymetry, sediments composition of the seafloor, sound speed profile (ssp), transducer beam pattern, and evolution of the surface waves. The drawback of using ray tracing in simulations of underwater networks composed by many nodes is the high computational complexity: a good trade-off can be using analytical models that takes into account multiple paths [60, 62, 67], at the price of a lower accuracy.

4.2 Underwater Acoustic Noise and Signal to Noise Ratio

When predicting the transmission range, the acoustic noise should be considered as well. Also, the acoustic noise depends on the signal frequency, and according to [60] it is composed by four main components:

- (1) the turbulence noise N_t , that influences only the very low frequencies, i.e., the frequencies below 10 Hz: its power spectral density (p.s.d.) in dB re μPa per Hz can be computed as:

$$10 \log N_t(f) = 17 - 30 \log f; \quad (4)$$

- (2) the noise caused by distant ships N_s is the dominant noise component for frequencies between 10 and 100 Hz, and its p.s.d. can be computed as:

$$10 \log N_s(f) = 40 + 20(s - 0.5) + 26 \log f - 60 \log (f + 0.03), \quad (5)$$

where s is the shipping factor that ranges between 0 (low shipping activity) and 1 (high shipping activity);

- (3) the noise caused by the wind-driven waves N_w is the most dominant noise component for the frequencies between 100 Hz and 100 kHz, and its p.s.d. can be computed as:

$$10 \log N_w(f) = 50 + 7.5\sqrt{w} + 20 \log f - 40 \log (f + 0.4), \quad (6)$$

where w is the wind speed in m/s;

- (4) the thermal noise N_{th} is the main cause of noise for frequencies above 100 kHz, and its p.s.d. can be computed as:

$$10 \log N_{th}(f) = -15 + 20 \log f. \quad (7)$$

The overall p.s.d. of the noise $N(f)$ can be computed adding the all noise components. Finally, observing the p.s.d. for the central frequency of the receiver f_c and taking a narrow band δf_c around f_c where the p.s.d. of the noise and the signal attenuation $A(d, f_c)$ can be considered as constant, we obtain

$$N = N(f_c) \cdot \delta f_c. \quad (8)$$

Given noise N , transmission source level P_{TX} (expressed in dB re μPa @ 1 m from the source) transmission range d , central frequency f_c and the signal attenuation $A(d, f_c)$, the Signal to Noise Ratio (SNR), in dB, can finally be computed as

$$\text{SNR} = 10 \log \frac{P_{TX}}{N(f_c) \cdot \delta f_c} - A(d, f_c). \quad (9)$$

Using this model, and defining as communication range the distance between the transmitter and the receiver where $\text{SNR} = 10$ dB, we obtain the plot in Figure 3, where we can observe how the communication range changes with the central frequency in case of no multipath, $s = 1$ and $w = 10$ m/s. The transmitter is configured with a transmission source level of 170 dB re μPa @ 1 m,

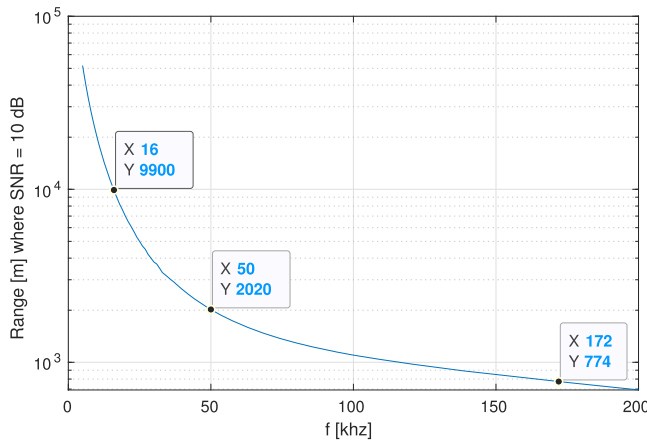


Fig. 3. Range of an acoustic vertical link computed with the model in [60] by varying the central frequency. The range is selected as the distance between the transmitter and the receiver where SNR = 10 dB.

bandwidth equal to half the central frequency; for simplicity, noise and signal attenuation are assumed to be constant in all bandwidths.

While the aforementioned empirical model is considered a good approximation for vertical links in generic scenarios, additional noise sources should be taken into account in certain areas. Snapping shrimps, for instance, becomes the dominant source of noise for the frequencies above 2 kHz in warm water scenarios [68]. Conversely, the noise caused by ships' propellers and engines becomes the dominant cause of noise for the frequencies below 20 kHz in port areas [69]. Finally, in the Arctic, the acoustic noise is well correlated with wind speed, because when sea ice deforms or fractures due to wind, waves, or currents, it produces loud sounds resulting in high acoustic noise, even down to bandwidths usually dominated by shipping traffic [70, 71]. For this reason, scientists prefer to measure the noise level in the field instead of using mathematical models, when possible [72].

4.3 Propagation Delay and Communication Stack

While in radio terrestrial networks the propagation delay is often negligible compared to the time needed for the data transmission, in underwater acoustic networks this is not true, as the signal propagates underwater with the speed of the sound, that is, on average, 1500 m/s,¹ i.e., five order of magnitude smaller than the speed of radio waves in the air. The result of this phenomena is the high transmission latency: in fact, the reception of a signal transmitted by a node that is deployed 1.5 km far from the destination starts 1 s after the beginning of the signal transmission from the source. The clear limitation of such channels makes low latency transmissions impossible, therefore real-time alarms and all applications with stringent low-latency requirements cannot be enabled by acoustic transmissions. Another limitation imposed by the high propagation delay is the impossibility to use terrestrial carrier-sense based Media Access Control (MAC) layers [83] such as Carrier-Sense Multiple Access (CSMA). Indeed, listening to an acoustic channel before transmitting does not guarantee to prevent packet collisions at the receiver. Also, the use of slotted MAC is not that effective, as Time-Division Multiple Access (TDMA) would require to insert a large guard time between slots to prevent collisions between packets transmitted in the same time frame [83]. On the other hand, when designing MAC layers for underwater acoustic networks, the

¹The speed of sound changes depending on water salinity, temperature, and density.

Table 2. Representative Studies of Underwater Acoustic Communication

Types	Key Points	Representative Works	Details
Analytical channel model	<ul style="list-style-type: none"> low complexity; accounts for channel geometry and acoustic noise; sometime very specific for some areas (e.g., shallow water, warm water, etc.); do not take into account for bathymetry and sediments compositions. 	Thiele [61]	One path propagation model validated in the Baltic and North Sea.
		Stojanovic extension of Urick/Thorp [60]	General model that takes into account channel geometry, colored noise and attenuation. It also takes into account secondary paths.
		Chitre [62]	Propagation model validated in the Singapore Sea, taking into account multipath and acoustic noise also caused by snapping shrimps.
		Roger [67, 73]	Considers an approximation of the ssp in shallow waters and accounts for power losses affecting the components of the sound field that bounce off the bottom one or multiple times. It provides a good accordance between simulations and at-sea experiments in shallow water scenarios.
Ray tracing based channel model	<ul style="list-style-type: none"> accounts for channel geometry and acoustic noise; very accurate: they predict the propagation behavior given the channel properties; they take into account for bathymetry, ssp and sediments compositions; computationally expensive. 	Bellhop [66]	The mostly used ray tracer to date, integrated in many network simulators, it takes into account ssp, bathymetry, sediments composition, transducer geometry and surface waves evolution.
		RAYLAB [64]	Considers sound speed profile and sediments composition of the seafloor. Some simplifications entail a lower complexity than other ray tracers.
		SIPSI/MOCASSIN and MOCMULTI [65]	Very accurate models for the Baltic Sea. In the case the environment is not represented accurately, the model may yield to unsatisfactory results.
Underwater network simulators and emulators	<ul style="list-style-type: none"> able to simulate large networks accounting for signal interference, propagation loss and propagation delay; provide good scalability to simulate a large number of nodes; some of them include a ray tracing model; some frameworks are totally opensource [74–78], others provide a free version for basic operations and an advanced version for which you need to pay [79, 80]. 	Aquasim [77], UAN [75]	ns-3 based simulators.
		ASUNA [76]	Matlab framework to simulate networks with link quality evolution based on real field measurements.
		WOSS [78]	ns-3 and ns-2 miracle based simulator to include realistic acoustic propagation modeling (e.g., the Bellhop ray tracer). It can be integrated to UAN, DESERT and SUNSET
		DESERT [74], SUNSET [79]	ns-2 miracle based simulators and emulators with capability of real field experimentation.
		UNETstack [80]	Java and Julia framework to simulate and test software defined modems and networks.
Underwater network test-beds	<ul style="list-style-type: none"> provide the possibility to perform sea tests of underwater networks; long term deployed test-bed; accessible to the scientific community upon request and/or specific agreement 	LOON [81]	Littoral testbed equipped with modems of different manufactures and capability of retrieve raw channel measurements.
		SUNRISE Testbed Federation [82]	Federation composed by 5 testbeds with static and mobile nodes for experimenting acoustic networks and navigation systems.

large propagation delay can be exploited to perform simultaneous transmissions still preventing collisions at the receiver [84, 85].

Another issue introduced by the communication latency is the difficulty to perform handshakes and establish connections between nodes without strongly reducing the network throughput, and for this reason transport protocols like Transmission Control Protocol (TCP) are not used. In

addition, the low transmission rates impose to use small headers to minimize overhead introduced by the communication protocols. For instance, the addressing of underwater nodes is not performed using Internet Protocol (IP) addresses [86], but by simply enumerating the nodes of the networks. In networks where a large number of nodes is envisioned, a more sophisticated addressing system can be used, for example, by grouping the nodes in clusters and enumerating only the nodes of a cluster [86].

With these considerations we can understand how important it is to perform an accurate design of an underwater acoustic network, not only selecting carefully the physical layer, but also developing MAC and routing layers that take into consideration the limitations imposed by the acoustic channel. For this reason, in the last ten years several underwater network simulators and test-beds have been developed [74–77, 79–81, 87] to help researchers and industries evaluating the network performance before the actual deployment.

4.4 Common Acoustic Modems

The most common acoustic modems developed to date can be divided into three categories as follows:

Low Frequency (LF) acoustic modems, whose carrier frequency is below 20 kHz, are characterized by a low bandwidth (usually below 10 kHz), a bitrate of about a few hundreds of bits/s, and a long transmission range, that can easily achieve a few tens of kilometers [88]. Given this frequency and bandwidth, and therefore the long wavelength, an LF acoustic modem is composed of large acoustic transducer (aka, the “antenna” of the acoustic modem) with a diameter that can easily exceed 15 cm, and weights at least a few kilos. LF modems can easily exceed a power consumption of 40 W when transmitting, and are the mostly used by the navy for surveillance and Mine Countermeasure (MCM) applications [89]. Due to their weight and power consumption, they are usually deployed from big assets, such as ships, manned submarines, large Autonomous Underwater Vehicles (AUVs), work-class Remotely Operated Vehicles (ROVs), and large mooring systems. The JANUS NATO standard [90] for first contact and interoperability between modems of different manufacturers, focus on the LF bandwidth.

Medium Frequency (MF) acoustic modems, whose carrier frequency is between 20 and 50 kHz, are usually characterized by a bandwidth between 10 to 20 kHz, a bitrate of about a few kb/s, and a transmission range of a few kilometers [91]. In this frequency and bandwidth range, an MF modem diameter typically varies in between 3 and 8 cm, and usually weighs less than 1 kg. Also, MF modems can easily exceed a power consumption of 40 W when transmitting, and are the most used on-board inspection class AUVs and ROVs for vehicle telemetry and localization [92], due to the fact of their smaller size, compared to LF modems, that simplifies the integration in medium size unmanned vessels, still enabling a considerable long range communication link. Given their extended use in AUVs that can be used for MCM applications, the JANUS NATO standard is in the process of being extended to also include the MF acoustic bandwidth [93].

High Frequency (HF) acoustic modems, whose carrier frequency is above 50 kHz, are usually characterized by a bandwidth greater than 20 kHz, a bitrate of few tens of kb/s (up to more than 100 kb/s for some devices [94, 95]), and a transmission range of a few hundreds of meters [96]. Given the high frequency, an HF modem is composed by a small transducer with a diameter of less than 3 cm, that usually weighs less than 100 g. Although transducers with this size usually cannot support high power transmission and are not rated for more than 1,000 m depth, they are very easy to handle due to their small size and weight. For this reason, most HF modems do not consume more than 20 W when transmitting, and are the most used on-board those small and micro AUVs and ROVs designed to be deployed from working boats without the need of winch and crane [97, 98]. They are usually used for high speed communication to download the data

collected from a vehicle during its mission when it is in the proximity of a base station or a surface sink [99]. A summary of the representative studies of underwater acoustic communication is given in Table 2.

4.5 Understanding the Underwater Acoustic Communication Characteristics through Measurements

We now discuss the underwater acoustic communication characteristics from real field measurements. Given the variability of an acoustic channel, it is not easy to predict whether an acoustic link will be stable or not. For instance, in the '40s researchers faced the phenomenon when an acoustic link between two nodes was established and stable during the morning, and not established at all during the afternoon: this “afternoon” effect [63] was caused by the change of the ssp gradient that was causing shallow zones in the afternoon, i.e., zones where the signals do not propagate.

In other environmental conditions a link may be stable for a few hours, then lost for one hour, and, finally, established again. This can happen, for instance, when a ship travels close to a node [100], or due to the high activity of marine fauna, or due to changes on current, wind and weather conditions (e.g., the presence of rain). The work in [101] demonstrates how a two states hidden-Markov model well describes this phenomena, where the transition between the state good channel and the state bad channel is computed by analysing real data. Specifically, this model has been validated by using the data of the SubNet'09 sea trial, organized off the eastern shore of the Pianosa Island, Italy. Many experiments were conducted, lasting up to ten hours and involving several thousand JANUS packet transmissions, at different times of the day and on different days along the summer season. The data used to validate the model was retrieved between the end of May and the end of August 2009, and includes more than 12,000 transmissions. Along with the acoustic measurements, also the environmental conditions such as wind speed, ssp, and temperature were measured.

A hybrid Automatic repeat request (ARQ) system can help dealing with the high instability of the channel [102], however, in the case the link is definitively lost, other solutions should be foreseen. For instance, instead of using a static routing, a flooding-based routing or a routing system that periodically checks whether a link exists, or that uses implicit Acknowledge (ACK) to check if a packet is correctly forwarded to a destination, can provide significant help, as demonstrated in the RACUN project with both simulations [89] and sea trials [103]. Another solution would be to employ multiple acoustic bandwidths, in order to use the one that best propagates to the destination in the given conditions, and to use the Modulation and Coding Scheme (MCS) that provides the highest throughput for that channel [93]. The authors in [104] demonstrates both via simulations and with a lake test in Germany the effectiveness of multimodal routing protocols in hybrid acoustic networks whose nodes are equipped with LF, MF, and HF acoustic modems. Five different topologies of a network composed by six nodes were tested. The same authors in [105] demonstrate with a sea trial in Hadera (Israel) how a multimodal MAC layer can provide significant benefits as well: the multimodal MAC was successfully tested in two topologies with four nodes. The modems used in the Hadera Sea trial are presented in Figures 4(a) and 4(b); specifically we used:

- 3 Evologics S2C 7/17 acoustic modems, used in nodes 1, 3, and 4, that are able to transmit at a maximum bitrate of about 7 kbits/s up to 7 km, according to the manufacturer, using the bandwidth 7-17 kHz. One S2C 7/17 transducer can be observed in Figure 4(a).
- 2 Evologics S2C 18/34 white edition acoustic modems, used in nodes 2 and 4, that are able to transmit at a maximum bitrate of about 13 kbits/s up to 3.5 km, according to the manufacturer, using the bandwidth 18-34 kHz. One unit of this modem can be observed in the bottom part of Figure 4(b).

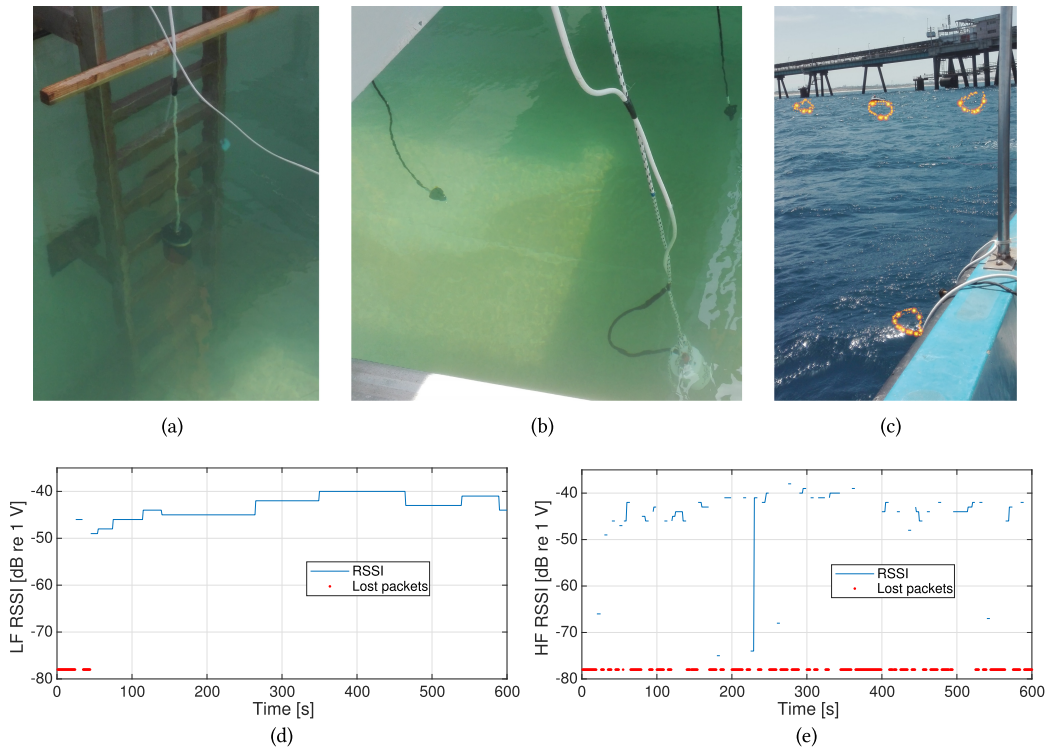


Fig. 4. The modems used in experiment in Hadera, Israel: (a) EvoLogics S2C 7/17 LF transducer, (b) two EvoLogics S2C 48/78 HF transducers (in the top) and one EvoLogics S2C 18/34 white edition MF modem (in the bottom of the figure). (c) presents a photo taken during the sea experiment: one node was deployed from the working boat (in the bottom), another node from a rubber boat (placed in the top-center of this picture) and two nodes were deployed from the Hadera electrical pier, long 2 km. Temporal evolution of the Received Signal Strength Indicator (RSSI) from node 1 to node 3 experience in Hadera for the (d) LF and the (e) HF link.

- 3 Evologics S2C 48/78 acoustic modems, used in nodes 1, 2, and 3, that are able to transmit at a maximum bitrate of about 30 kbits/s up to 1 km, according to the manufacturer, using the bandwidth 48-78 kHz. Two S2C 48/78 transducers can be observed in the top part of Figure 4(b)).

Figure 4(c) presents a photo taken during the test from the working boat used to deploy node 3. Node 1 was deployed from the rubber boat in the top-center of the figure, while nodes 2 and 4 were deployed from the pier. The distance between nodes was, on average, 250 m, and the nodes were deployed at a depth of 1 m. The water depth was about 25 m.

The time evolution of the LF and HF links between node 1 and node 3 can be observed in Figure 4(d)-(e) (the nodes were not equipped with MF modems). The red dots indicate when a transmitted packet would have been lost due to bad channel conditions, while the blue line presents the time evolution of the Received Signal Strength Indicator (RSSI) of the received packets. The RSSI, provided directly by the modems, indicates the received signal level in dB re 1 V and represents the relative received signal strength, i.e., higher RSSI values correspond to stronger signals. In this scenario we can observe that, while the HF link was not stable mainly due to the strong wind that was causing large waves and significant noise to the HF bandwidth, the LF link was very robust:

however, the higher transmission speed of the HF link entails that, in order to achieve a higher throughput, the HF link should be used as soon as it becomes available.

In another test performed by the University of Padova and mentioned in [106], instead, a multimodal LF and HF acoustic network was deployed 40 m far from a cargo ship docked in the port with the engines turned on. With these conditions, where the noise is predominant in the LF bandwidth, the LF modem reached only the same transmission range of a HF modem. Moreover, the HF link was more stable because the noise level caused by the cargo ship engines was very close to the saturation level of the LF transducer, while the HF transducer was almost unaffected by this low frequency noise.

In both tests, however, the transmission range declared by the modem manufacture was not achieved: the main reason was due to the fact in both cases the transducers were deployed only 1 m below the sea surface, thus the reception was strongly affected by multipath reflections with the sea surface.

Both multimodal routing and MAC were tested using the DESERT underwater framework [74], and they both demonstrate how using multiple technologies in the same node can provide a significant gain in terms of performance and reliability compared to single technology systems, paving the way to further studies and development of agile network architectures, such as the one performed by [93].

4.6 Practical Considerations

Despite that the physical model of acoustic propagation presented in Section 4.1 and 4.2 states that, in general, the lower the carrier frequency, the longer the transmission range [60], this may not be true in some specific cases, as the acoustic communication can be strongly affected by seafloor composition, multipath reflections, environmental conditions, and shipping activity. Specifically, LF signals are strongly influenced by shipping noise [69], because the noise caused by ships' propellers and machinery is below 20 kHz. Conversely, HF signals are strongly affected by the noise caused by wind waves, rain, and snapping shrimps. For this reason, in a port in the proximity of a cargo ship with the machinery on, it is not rare to achieve a longer range transmission with HF signals than with LF signals, as the LF receiver would be very close to saturation and receive a signal with a very low SNR. In addition, the multipath caused by signal reflections with the seabed and with the water to air boundary can strongly deteriorate the signal, thus limiting the transmission range. For this reason, most of commercial systems employ frequency hopping to mitigate the multipath effect, thus limiting the transmission rate to the benefit of a more stable communication link. Vertical transmissions (e.g., performed between a node deployed close to the sea surface and a node deployed close to the sea bottom) instead, are less prone to multipath, and the authors in [107] demonstrated that broadband communications can be performed with MF signals at a distance of several kilometers.

In the case the communication geometry and the node position is known in advance, transducers with directional beam pattern can be used rather than omnidirectional or hemispherical transducers, in order to concentrate the transmitted power in a certain direction, and hence extend the transmission range and reduce the multipath. Conversely, if the network is composed by mobile nodes that are performing a path that is unknown before the deployment, an omnidirectional transducer should be employed. Information about the transducer beam pattern is always specified in the modem's data-sheets provided by the manufacturer, e.g., [91].

Another aspect that can strongly impact the reception of an acoustic signal is the Doppler effect caused by the movements of the submerged nodes. This aspect should be taken into account not only when mobile nodes, such as AUVs and ships, are used, but also when static nodes are deployed from buoys and mooring systems, as they may drift due to both water current and wind. The

Table 3. Acoustic Communications Advantages and Disadvantages

Advantages	Disadvantages
Long range (up to 30 km)	Low rate (up to 10s of kbps)
Robust in deep water vertical links	Poor in shallow water horizontal links
No need for line of sight	Strongly affected by multipath
Availability of good channel models and network simulators for simulation purposes	Affected by acoustic noise
	High latency
	May impact marine life
Can be combined with ranging and positioning devices	Can interfere with other manufacturers' positioning devices and sonars
Several products available in the market	Affected by sound speed gradient and nodes' mobility (Doppler)

Doppler effect leads to frequency shift when at least one of two communication partners is moving. The frequency shift Δf of a signal with frequency f_s sent by a node moving at speed v_s to a node moving at speed v_r in the opposite direction can be computed as [108]

$$\Delta = f_s \frac{v_s - v_r}{c - v_s}, \quad (10)$$

where c is the speed of sound underwater. For example, a 75 kHz signal sent between two AUVs moving at 2 m/s in the opposite direction will be shifted by 200 Hz [109]. One possibility to prevent this issue is to improve the separation of the adjacent frequencies and then use a long preamble to estimate the Doppler spread right before the payload signal is received, at the cost of a lower data rate.

In order to predict the quality of the acoustic link in a certain area, also the period of the year should be taken into account, not only to consider the acoustic noise specific of that period (e.g., caused by marine mammals migration, high activity of marine fauna like snapping shrimps, strong wind often observed only in some specific periods of the year, etc.), but also the sound speed gradient along the water column. Specifically, the sound of speed underwater changes that depend on salinity, temperature and pressure. Although the salinity of a certain area can be considered constant in a determinate period of the year, both pressure and temperature change considerably along the water column, and so does the sound speed. Depending on the period of the year, temperature and salinity can change significantly, and so the ssp observed in the summer can be significantly different than the one experienced in winter. This variation can cause significant changes in the acoustic propagation, and thereby should be taken into account as well.

Acoustic signals are also used in the underwater domain to perform ranging and positioning between underwater nodes (e.g., with long and short baseline devices [110]), to measure the sea depth below and in front a ship (e.g., with single, multibeam and forward looking sonars [111]), and to measure the speed of an underwater vehicle (e.g., with a Doppler Velocity Logger (DVL) [112]). While an acoustic modem can integrate positioning and ranging capabilities at the price of a small reduction on the communication throughput [91, 110], their signal may interfere with the one used by other manufacturer's ranging, sonar and DVL devices: for this reason, an acoustic modem cannot be deployed in underwater assets without first analyzing whether the modem interferes with the other acoustic tools already installed in that area, i.e., by checking if the modem overlaps in frequency with the other devices. Table 3 summarises the advantages and disadvantages of acoustic communications for UWSNs.

4.7 Future Research Challenges

Due to the large uncertainties of the underwater channel presented in Section 4.4, a transmission scheme that outperforms all others in each underwater channel does not exist, but for each acoustic channel we can identify which frequency, bandwidth, modulation, and coding scheme should be employed to obtain the best performance possible. For this reason, the current trend, when designing an underwater network, is to add multimodal capabilities to the nodes, equipping them with multiple transducers working at different frequencies [105], and able to change MCS according to the quality of the underwater links [93]. For example, a frequency hopping waveform should be used when multipath is in place to limit intersymbol interference (ISI) at the price of a lower data rate, and a robust MCS should be used in the case of low SNR. Conversely, frequency hopping shall not be used for vertical transmissions, and a faster MCS can be used to achieve a high data rate in case of high SNR. A further step in the direction of multimodality and adaptivity can be performed by combining different communication channels, i.e., using acoustic, optical and electromagnetic modems in the same node, in order to get the best of each technology [113, 114].

Despite the mission-critical applications where underwater acoustic networks are used (e.g., surveillance, anti tsunami system, MCM, etc.) security aspects of underwater acoustic networks have still not been deeply investigated so far [115]. The countermeasures to Denial of Service (DoS) attacks used in wireless terrestrial networks cannot be directly applied to the underwater domain due to the lack of resources in terms of data rate and latency, therefore solutions specifically designed for underwater environments need to be developed. Some analytical and simulation studies have been performed in [100, 116, 117] and [118] to propose countermeasures to jamming and replay attacks, but the results have not been yet proven in a sea experiment. Other types of DoS attacks also need further investigation [115].

The high power consumption and the high cost of traditional commercial acoustic modems (typically used in military and offshore applications, where a unit can easily exceed 8K US Dollars), make their use in civilian applications prohibitive. With the introduction of new sensor technologies applicable to smart ports [99] and aquaculture sites [119], both industrial modem manufacturers [120] and research institutes [109] have started the development of low-cost and low power acoustic modems for coastal deployments. Indeed, the requirements of these applications in terms of communication range and data rate are more relaxed than the one needed for surveillance and offshore applications; instead, they require an affordable device that can be powered with small batteries. New products start becoming available, all characterized from a cost of less than 1,000 US Dollars, a power consumption of approximately 1 W, and are able to transmit up to a few hundred meters at a data rate of few tens [120–122] or few hundreds [109, 123] of bits per second.

Finally, an application that so far has only been partially enabled by acoustic communications is the possibility to perform underwater video live streaming in real time. Despite that several researchers have invested a great deal of effort proving the feasibility of such an application [95, 107, 124], the results proved that still-images and very-low quality video can be transmitted through the acoustic channel either in close range [95, 124], or in very favorable conditions [107]. Nevertheless, in short range, high-quality videos can be streamed in real time with other communication technologies, such as the optical modems described in the following section.

5 VISIBLE LIGHT UNDERWATER COMMUNICATIONS

Visible light communication (VLC) has been standardized by IEEE in 2011 in the form of IEEE 802.15.7 with a data rate target of 100 Mb/sec line-of-sight communications in clear media. Several survey articles have recently appeared on VLC [125–127]. In [125] the authors discussed the physical layer techniques such as modulation and circuit design in the context of VLC, whereas the

authors in [127] studied different networking aspects such as sensing and medium access protocols of VLC. Various applications of VLC are reported in [126]. Recent works have shown the feasibility of about 300 m underwater communication range using laser optical wireless communication [5].

This section has been organized as follows: We first describe the signal propagation characteristics of optical signals in underwater medium as a background overview in Section 5.1. We next discuss various existing simulation and experimental platforms/modems in the area of underwater optical communication in Sections 5.2–5.3. We also provide an experimental measurement study for underwater visible light communication in Section 5.4. Finally, we articulate the open challenges and discuss key research questions that remain to be solved in underwater optical wireless communication in Section 5.5.

5.1 Propagation Characteristics of Underwater Optical Communication

Optical wavelengths in the range of Blue, Violet, and Ultra-Violet have very low attenuation underwater, compared to other visible light wavelengths and radio frequencies. This has initiated much interest in using optical wireless communication through VLC in underwater applications. In pure water the light absorption is a minimum at 400–550 nm of the visible spectrum, however, such absorption characteristics change based on the amount of phyto-plankton species and dissolved organic matters in the sea water. Other than absorption, underwater scattering due to density fluctuations, organic and inorganic large particles also impacts the performance of UWOC. Also, the performance of VLC greatly deteriorates in the presence of obstacles such as marine species.

Today, there is no standardized channel model for underwater optical wireless communication, which has opened up opportunities for physical layer modeling works in this space. However, works so far have largely extrapolated from fundamental visible light communication (VLC) channel model [128] in air medium, where the VLC channel is primarily defined by the optical channel DC gain. Thus, conceptually, the VLC channel [128] can be represented as

$$y = (h)x + n \quad (11)$$

where x and y denote transmitted and received signal intensities, respectively, h is the channel gain, and n denotes the channel noise. This model is extrapolated for underwater medium as,

$$y = \alpha(h)x + n \quad (12)$$

where, α represents the effective signal power loss due to underwater medium (due to various effects such as scattering, absorption, and reflection). Underwater optical wireless communication concept is studied extensively in several survey articles [5, 129, 130], which have presented various extrapolations of the fundamental underwater VLC channel model in Equation (12).

5.2 Experimental Underwater Optical Communication Systems/Modems

We now discuss the well-known VLC modems and underwater experimental platforms, as well as simulations/studies that model the performance of these modems.

5.2.1 Aqua-Fi. In an attempt to bring the Internet to an underwater environment, an underwater wireless optical system, known as Aqua-Fi, was tested using LED and laser as the medium of data communication. The Aqua-Fi system proposes a low-power, cost-effective multihop communicative piece of technology that requires very little underwater infrastructure, proving it to be practical and flexible [131].

One positive feature of this underwater network solution is the way in which handheld mobile devices can function and operate freely in the underwater environment. Text messages and multimedia are first delivered to a gateway attached to the diver and then from the gateway to other

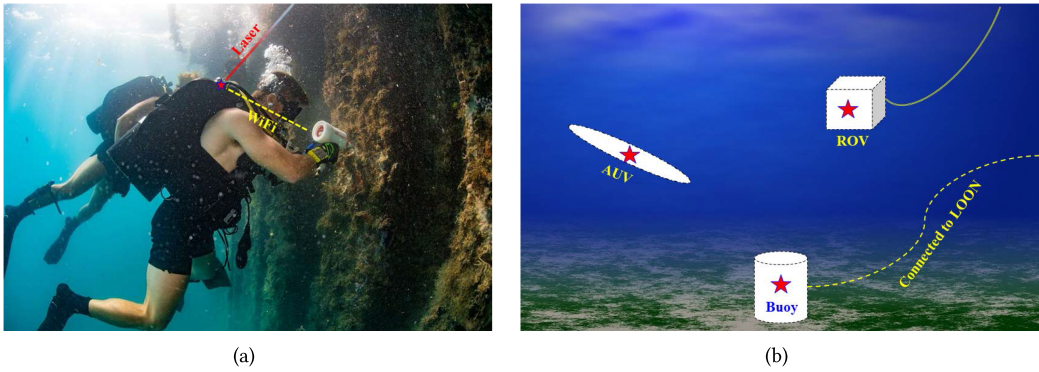


Fig. 5. System overview of (a) Aqua-Fi [131] and (b) OptoCOMM [133]. The figures are adapted from [134, 135].

nearby devices (such as a ship's receiver) while remaining underwater. It is this level of flexibility that makes Aqua-Fi such a unique proposed system of communication. To achieve network flexibility, high bandwidth is necessary. Therefore, RF wireless links, which are most effective in short ranges [9, 132], are implemented to connect the underwater mobile device to the gateway strapped to the diver's back. After receiving the RF signals, the main gateway relays the data to the nearest receiver (connected to a ship) via laser or LED transceivers. After the ship's receiver acquires the LED or laser transmission, any terrestrial-based or satellite connection to the Internet can be used. The system overview of Aqua-Fi is depicted in Figure 5(a).

For this UWOC platform, the goal is to relay signals using both LEDs and lasers depending on the distance from the ship's receiver. In essence, if the gateway is less than or equal to ten meters away from the ship's receiver, LED transmission is ideal; otherwise, laser transmission is necessary in order for the visible light to reach the receiver without suffering from excessive attenuation. With respect to the LED system in Aqua-Fi, it is built in conjunction with a Raspberry Pi 3B. Regarding the software implemented with the Raspberry Pi, **Point-to-Point Protocol (PPP)** is used to modulate **on-off keying (OOK)** for the optical signal, and the Raspberry Pi relays packets from the PPP interface to the Ethernet Internet. The Aqua-Fi laser system is very similar to the LED system although the LEDs are replaced with SN-LDM lasers. Although the laser system requires more power, it results in a higher data rate of 1 Mbps as well as a wider range of travel, thus allowing Aqua-Fi to operate at greater depths. Similar to the LED system, the laser system also employs OOK modulation for transmission. It has been measured that under ideal conditions with multiple parallel streams or transmission, Aqua-Fi can reach a data rate of 17 Mbps before experiencing packet loss. It was also measured that latency can range between 1 and 85.5 ms depending on how much stress the system is under.

In terms of limitations and drawbacks, one glaring issue is the need to manually adjust the receiver amplifier to be nearly perfectly aligned. When this system is deployed in the ocean, natural and seemingly negligible turbulence can hinder the alignment of Aqua-Fi components. Another drawback has to do with the low data rate considering that optics is known for its high data rates. Recent studies of maximum underwater optical data rates have shown that rates can reach well into the order of gigabits per second [136]. The lackluster data rate is likely due to the use of the Raspberry Pi since its primary use is not for data communication and transmission. Rather, if the Raspberry Pi were replaced by an interface module dedicated to data transmission, such as an SFP transceiver, data transmission for Aqua-Fi could see rates on the order of 10^9 instead of 10^6 .

5.2.2 OptoCOMM. OptoCOMM [133] is another underwater optical wireless modem designed for short-range high-speed communication. OptoCOMM is claimed to be fully compatible and integrable with the LOON testbed [137] of the SUNRISE platform [82, 138] located on the Gulf of La Spezia. It provides SUNRISE with a more expansive toolkit for its users that stretches beyond just acoustic experimentation. The OptoCOMM project has developed three types of modems to be integrated in the LOON testbed. One of the modems can be directly anchored to the seafloor, meaning it would be connected to the LOON infrastructure itself. The second modem is battery-powered and can be connected to an external device such as an **Remotely Operated Vehicle (ROV)** [139]. The third modem variation is meant to be mounted onto the eFolaga AUV that is already present in the LOON testbed. The system overview of these three types of modems is shown in Figure 5(b).

Various factors, such as the refractive index and attenuation coefficient, can limit the maximum transmission range of underwater optical modems. Achieving a wide transmission range is even more difficult in the LOON testbed because the La Spezia harbor is characterized by very turbid water with inconsistencies in turbulence and salinity [133]. As a result, the effective range at which the OptoCOMM modem can transmit LED light cannot exceed 10 meters in most conditions.

With respect to the design, OptoCOMM modems are optimized to be most efficient in shallow waters. Furthermore, in an attempt to reduce the manufacturing cost, only one **Avalanche PhotoDiode (APD)** is used to make the modem. Another helpful feature of the modem is an initial handshake phase that ensures that the receiver is aligned correctly and that a secure connection to the LED transmitter is established. Regarding the modem software, the modems are developed to be integrable with the SUNSET framework [140], as the framework acts as the middleware between the optical modems and the LOON testbed infrastructure. Using TCP/IP protocol, the user can access the modem's status as well as set and retrieve settings via an Ethernet interface. This transmission protocol was tested in a preliminary test [133], which deduced that data could be successfully transferred even with underwater obstructions that caused contrasting data.

The concept of OptoCOMM is an extremely forward-thinking idea that can change the way in which underwater field-level testbeds and platforms operate. The OptoCOMM project has designed three relatively inexpensive modems that can be used slightly differently in the LOON testbed in the Gulf of Spezia. This provides the researchers of the testbed a level of flexibility, in both optics and acoustics, that is rarely seen with sea-level experimental platforms. OptoCOMM is still, however, a new piece of technology that can be improved. One of the limitations of OptoCOMM is the limited effective transmission range of 10 meters and an average bitrate of 10 Mbps.

5.2.3 Performance Modeling of Optical Modems. It is evident that UWOC devices, particularly modems, perform differently depending on various factors such as turbidity, transmitter alignment, and external background light. The experimental endeavors in [141] attempt to model the performance of underwater optical modems by using a database of modem performance figures in order to match the nature of real optical transmissions. This helps to account for the fact that traditional propagation models, such as those influenced by the Beer-Lambert Law [142], do not perfectly model emission from LEDs or lasers.

The performance data and modeling that resulted from the experimentation is included in the DESERT underwater simulator [143, 144]. Data from underwater beam patterns helped the researchers in [141] to extrapolate the necessary statistics. For instance, the beam pattern from the BlueComm 200 optical modem [145], was utilized to define different bit rate levels for different depths in ideal water conditions. In [146, 147] the authors have designed a high bandwidth wireless optical communication solution, named AquaOptical. In this project, the authors have

designed three types of modems; a long range system, a short range system, and a hybrid. This communication system achieves a data rate of 1.2 Mbps at distances up to 30m in clear water, whereas in turbid water (visibility estimated at 3m) it achieves 0.6 Mbps at distances up to 9m.

Given the BlueComm 200 and MIT AquaOptical models, researchers in [141] were able to create a 3D representation of maximum transmission range by calculating the inclination angles that exist between the transmitter and receiver. It is important to note that these angles must be computed from both the transmitter and receiver's point of view, which also implies that the transmitter and receiver have their own respective rotation angles. The coordinates of the transmitter and receiver are used to obtain normalized attenuation coefficients that are crucial in modeling and simulating wave propagation and path loss. It has also been found that the difference in depth between the transmitter and receiver is another parameter important to modeling the maximum transmission range.

The researchers in [141] have taken an unorthodox approach to simulate UWOC devices in which a database of modem performance is built rather than solely implementing analytical laws and models. These researchers found that modeling based only on the Beer-Lambert Law is not sufficient for accurately portraying optical wave propagation, especially for LEDs and lasers. Additionally, the proposed model has been integrated with genuine field-level measurements, making it a flexible, expandable, and reliable modem. In terms of its implications for future underwater optical platforms, this model has brought attention to many factors that are often ignored in many simulators, such as outside ambient light and inclination angles from the point of view from the transmitter and receiver.

5.2.4 Other Experimental Assessment of Underwater Light Propagation. The researchers involved in [148] attempt to investigate the behavior of light propagation in underwater environments. Ray tracing software as well as a 1.2m-long water tube were used to help replicate the propagation of light. To emulate the different types of underwater environments (to replicate the clear ocean, coastal ocean, and turbid harbor), different amounts of sand were added to the water tube; this leads to three types of water with different attenuation coefficients. Using a laser as the source of light, the simulated software and experimental results were compared.

For the experimental setup, blue and green wavelengths were used since they are most appropriate for long-distance propagation underwater due to their lower absorption [149]. Within the water tube, an Nd:YAG laser [150] is used to produce a 532 nm wavelength to propagate through the water at a peak power of about 2.15×10^5 W. Simulation is carried out using the Zemax-ray tracing software [151] which tries to replicate the receiving telescope of the water tube and simulate the propagation of light. Each attenuation coefficient is considered by the Zemax software to calculate the power-level of the laser beam once it reaches the receiving end. Using the attenuation coefficient values, Zemax provides an illustration of the collected laser power by depicting the irradiance [148]. For the least turbid water, the collected laser power corresponded to about 54.4% of the laser source power. For the water with medium turbidity level, the collected power represented 31.4% of the source power, and for the water with maximum level of turbidity, the receiver received 17.3% of the original laser source power. Researchers also replicated highly turbid harbor water, which resulted in the Zemax software depicting a collected laser power that was 0.45% of the transmitted power, indicating that the laser through the highly turbid water had strongly attenuated. When comparing the experimental results to that of the Zemax-ray tracing software results, received laser power values were almost identical.

With experimental and simulation results generally agreeing with each other, it can be stated that the Zemax-ray tracing software has the ability to model and reproduce underwater light propagation in a very accurate manner. Although the experimental setup may not be scalable for

Table 4. Summary of Existing Experimental Underwater Optical Communication Systems

System Setup/Reference	Key Features
AquaFi [131]	<ul style="list-style-type: none"> flexible, low-cost, and low-power underwater network solution provides internet connectivity in static water environment limited range of communication
OptoComm [133]	<ul style="list-style-type: none"> compatible with existing acoustic modems 10m range in shallow medium/high turbidity harbour waters provides 10 Mb/s transmission rate
BlueComm 100 [152]	<ul style="list-style-type: none"> performs well in any ambient light condition smaller size; 1-15m communication range provides three data rates (1.25, 2.5 & 5 Mb/s) in different settings hemispherical shape enables communication link in multiple directions
BlueComm 200 [153]	<ul style="list-style-type: none"> long range optical modem (up to 150m) TDMA to provide a bi-directional high speed low latency link suffers with ambient lighting provides data rates up to 10Mb/s
BlueComm 200UV [154]	<ul style="list-style-type: none"> operates in UV spectrum with a visible spectrum filter maximum range of 80m data rates up to 10Mb/s
BlueComm 5000 [145]	<ul style="list-style-type: none"> can be mounted on an AUV (Autonomous underwater vehicle) provide 600Mb/s (upload) & 200Mb/s (download) data rates smaller range of communication (up to 7m); Depth ratings to 4,000m

underwater platforms and testbeds, the Zemax software has definitely proven itself a more than viable and reliable option for underwater simulation and modeling. In other words, [148] has demonstrated that Zemax can be considered as a candidate for underwater simulators, as its software could be integrated with other software-based simulators such as DESERT. Table 4 lists the existing modules/tools for conducting experimental underwater optical communication.

5.3 Robotic Simulation Platforms Relevant to Acoustics and Optics

One of the key aspects of underwater wireless networking is the placement and movement of underwater infrastructure, devices, and vehicles/robots. As in free-space wireless networking, movement of the wireless nodes in underwater medium also leads to different channel conditions that impact the quality of the communication link. Hence, underwater networking studies have to be fundamentally correlated with the mobility patterns of these wireless nodes. Also, since there are no clear pathways (e.g roadways, landmark routes and GPS assistance), the signal variations under mobility is random with a higher rate of changes. Hence, we also survey some of the works in mobility studies, particularly through simulation tools, to model, characterize, and potentially plan underwater mobility.

Autonomous underwater vehicles (AUVs) are programmable tools on which both acoustic and optical modems can be mounted. Therefore, platforms that are able to simulate AUVs and underwater robotic movements should be considered relevant to the advancement of underwater acoustics and optics. This section analyzes said simulators that can model AUVs and their movements.

5.3.1 UWSim. As an open-source project specifically designed for the simulation of underwater vehicles, UWSim employs graphics and modeling engines such as OpenSceneGraph [155] and the Bullet physics engine [156, 157]. In essence, many of the software packages included in this simulator allow users to precisely model underwater wireless sensor networks which, in turn, enables researchers to study their influence on the movement and general behavior of AUVs [158].

The Bullet physics engine in UWSim [158] provides precise collision detection between various shapes, meshes, and rigid bodies. Moreover, robotic features, such as arms, tracks, and wings can be attached to the vehicle, making UWSim a useful tool for a wide range of underwater robotic vehicles. These simulated robotics features can emulate physical interaction with the outside environment. The simulator also has the ability to model vehicle control and even simulate an AUV receiving data and sensor signals [159]. These signals include sonar, acoustic signals, and optical signals from underwater modems. UWSim can also simulate a plethora of sensors, such as pressure sensors, contact sensors, force sensors, and multibeam sensors [159].

In the recent introduction of UWSim's extension, known as UWSim-Net [158], many software packages and libraries were upgraded. For instance, UWSim-Net includes many NS-3 modules such as AquaSim [160] in order to better model acoustic modems. This particular feature allows the user to reproduce the performance and specifications of acoustic modems. On top of acoustic modem simulation, UWSim-Net contains generic models of VLC modems that can be configured in the simulation. The specific behavior of the simulated modems is defined by bitrate, intrinsic delta, jitter, and experimental measurements that can be inputted as parameters. This provides the researchers with the most accurate representation of underwater modems. The user-defined parameters can be specified in an XML file that UWSim-Net will interpret with ease.

Using UWSim in conjunction with UWSim-Net proves not only to be an effective way of simulating AUVs, but this combination also allows users to accurately simulate both acoustic and optical modems. The UWSim-Net extension provides much more flexibility in terms of which underwater factors and components can be parameterized. Furthermore, the extension software enables users to simulate packet loss, propagation delay, and communication delay which are crucial factors when carrying out underwater experiments [158, 159].

5.3.2 MORSE. The **Modular Open Robots Simulation Engine (MORSE)** [161] is another flexible open-source simulator created for the purpose of modeling robotic movements and 3-D environments. Maritime and underwater environments are included in MORSE's available environments, making the simulator relevant for underwater robotic visualization including but not limited to the modeling of AUVs. Similar to UWSim, MORSE is built upon the Bullet physics engine, but it also incorporates the Blender Game Engine [162]. Blender allows MORSE to better simulate three-dimensional movement and collisions among rigid bodies [161, 163]. Another advantage that Blender provides is a very high level of detail of 3-D models. Effects such as texturing, shading, and lighting are all at the user's disposal because of the Blender engine. Blender also comes equipped with a dedicated Python API that enables users to easily implement Python scripts and modules. Moreover, MORSE provides the user with an interface for interacting with MOOS software [164] that was originally created for the modeling of underwater autonomous robots. Therefore, MOOS can be seen as a type of middleware for which MORSE provides an interface.

Another relevant feature of the MORSE software is its ability to utilize actuator components that allow the configuration of properties such as linear and angular velocity as well as robotic position [159, 161]. On top of actuator configuration, various sensor components are included, namely collision sensors, battery sensors, laser sensors, depth cameras, and odometry sensors. MORSE's depth camera is similar to the UWSim depth camera; however, MORSE is able to generate a 3-D image, which is an improvement when compared to UWSim's 2-D depth camera performance [159]. MORSE also allows users to create custom sensor components, providing a great degree of flexibility for simulation. With respect to simulating an underwater environment, MORSE provides two default underwater environments with which to experiment although it is possible for the user to create custom environments. MORSE claims to have the computational power to simulate multiple robots in an environment [159], which implies that many AUVs, each with a different configuration, can also be experimented.

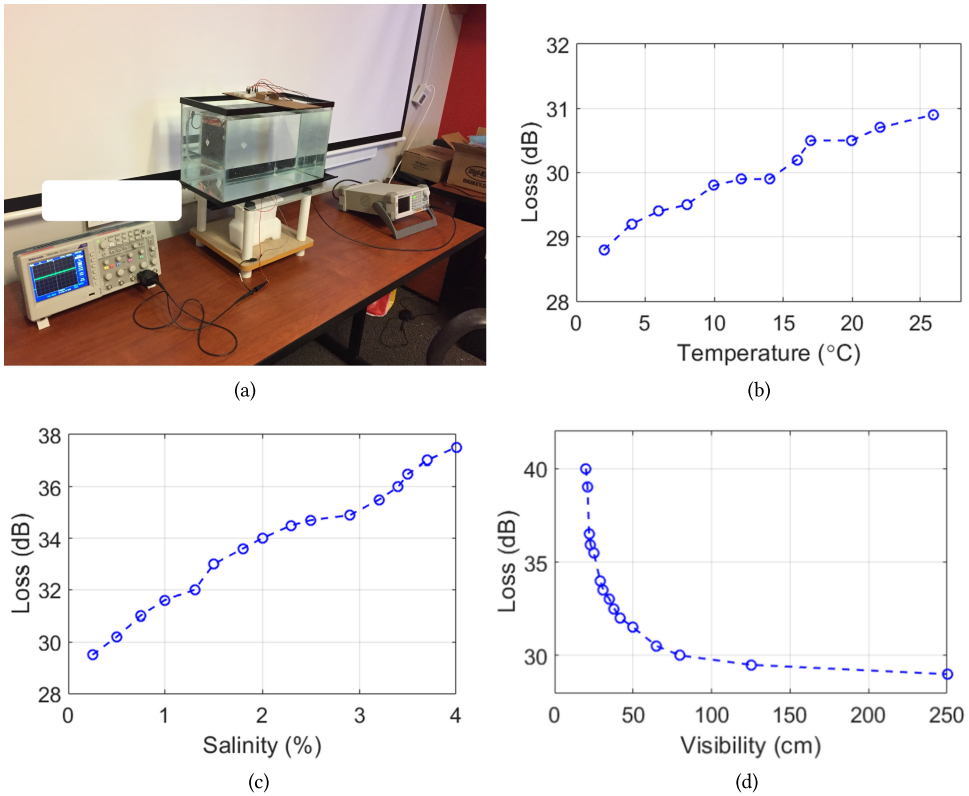


Fig. 6. (a) Experimental setup for characterizing underwater VLC. The setup includes 19 liters of clear distilled water in a 2ft depth fish-tank with 23inches of water medium. Variation of path loss with different (b) temperature, (c) salinity level, and (d) turbidity (measured as a function of visibility). Note that we have defined the loss function (Y axis) as the ratio of transmit power to receive power.

5.3.3 Gazebo. Another popular open-source robotic simulator known as Gazebo [165] is particularly relevant to acoustics and optics because of its versatility in which several physics engines such as Bullet and Simbody [166] are supported. Moreover, many packages including the **ROS (Robot Operating System)** package already come equipped with the simulator, and other third-party middleware can easily be incorporated with Gazebo. An example of the integration of Gazebo and middleware can be seen in [167] where Gazebo was integrated with the **Robot Construction Kit (ROCK)** software. The merging of these software packages have allowed researchers to construct a real-time AUV simulation by using the ROCK GUI packages to facilitate the 3-D representation of data models.

Gazebo offers many types of sensors including multicamera configuration, contact/collision sensors, and laser scanners. These sensors, when used with the various built-in hydrodynamic plugins [168], can help simulate an elaborate underwater environment. For instance, the **Digital Elevation Model (DEM)** [169] is a supported feature of Gazebo that allows for ocean floor texture to be imported as terrain. When coupled with Gazebo's contact sensors, intricate simulation with the AUV and its environment can be conducted. An example of this is introduced in [170] in which a set of third party packages including ROS applications and plugins allow underwater vehicles to be simulated in Gazebo with more detail and control. The proposal is referred to as the **Unmanned Underwater Vehicle (UUV) Simulator**. With AUVs being a specific type of UUV,

the UUV Simulator is especially relevant to the progression of underwater acoustic and optical platforms. Thruster configuration and model-based feedback is also included although these particular features are more relevant to ROVs. Even so, many field-level testbeds such as SUNRISE and OtpoCOMM make use of ROVs for real-time experimentation.

Gazebo as a standalone platform may seem lackluster; however, since it is adaptable, versatile, and flexible to a multitude of other plugins and packages, this platform proves to be an extensible tool for AUV simulation. One apparent limitation, however, is that there are no simple ways in which to model acoustic or optical modems. Unlike UWSim, which accommodates default modems for visualization, Gazebo does not provide a similar type of feature as of now.

5.4 Understanding the Underwater VLC Characteristics Through Measurements

In this section we present a preliminary measurement of underwater VLC characteristics; the experiments were conducted at MORSE Studio lab at Georgia State University [171]. A blue LED transmitter controlled by a function generator is used as a transmitter, whereas a matched photodiode is used as a receiver that records the analog power value on an oscilloscope. The experiment is conducted inside a 19-liter fish-tank as shown in Figure 6(a).

Figures 6(b)–(d) show the VLC path loss with the variation of temperature, salinity, and turbidity. We can observe that the path loss increases as the salinity increases. This is because the visibility decreases with increased salinity as the water becomes more foggy, and thus inducing more scattering and loss of signal power. The variation in signal strength with temperature is less pronounced. Our hypothesis for higher loss at high temperature is that, at higher temperature there is more molecular movement, thus requiring energy absorption from the optical beam. The absorption is lesser at lower temperature as the density is higher and the molecules are less mobile (activated). The loss of signal intensity with lower visibility is due to the higher scattering, therefore loss of signal power when more particulates are dissolved/colluded in the water medium.

5.5 Future Research Challenges

Underwater optical wireless communication, particularly using VLC, is relatively a new concept when compared with traditional underwater acoustic communication. However, the unique characteristics of VLC such as directional and thus less interceptible communication, possibility of long range with low latency (speed-of-light propagation), and off-the-shelf emitter and receptor components availability, make it a forefront runner for next-generation underwater networking. However, as any technology adoption requires extensive experimentation and testing, the key limitation in underwater VLC is the dearth of experimental platforms/infrastructure to conduct UWOC experiments. As can be inferred from the survey works in UWOC [172], there is a significant difference in the amount of theoretical works versus experimentation in UWOC. This is attributed to the challenges in setting up experimentation platforms for UWOC, as there is no set standard that can be easily replicated and thus prototyped and produced. This also creates a bottleneck for research as it limits repeatability, therefore making testing and replication of theoretical models and bounds infeasible.

Addressing these challenges calls for innovative approaches such as crowd-sourcing data from experiments conducted by independent research groups. This means that the community must be ready to share and open datasets that can be tested by other research groups and collaboratively improve model designs and infrastructure prototyping. VLC can also be combined with acoustic communication in a way to leverage the best of both worlds. In particular, the high-speed short range VLC links can be complemented by long-range reliable acoustic links for improving fidelity of underwater networking applications and potentially motivate new use-cases. While such ideas of hybrid underwater communication have been approached before (see Table 5), the dependency

Table 5. Summary of Existing Experimental Hybrid Underwater Communication Systems

Reference	System Design	Scope of Work
Fitzpatrick et al. [173]	Sonar + Laser	<ul style="list-style-type: none"> • scalable airborne imaging system of underwater • robust system in deep and turbid waters • tested in controlled and known water environments
Moriconi et al. [174]	Acoustic + FSO	<ul style="list-style-type: none"> • reliable (communication link) system design • improve data rates and stable connectivity in different water conditions
Chowdhury et al. [175]	RF + FSO	<ul style="list-style-type: none"> • Multi hop system design and maximizing system throughput • water environment sensing and real time data transmission • high power and data transmission efficiency
Vasilescu et al. [176]	RF + Acoustic + FSO	<ul style="list-style-type: none"> • both sensing and communication • consists of multiple sensor nodes called AquaNodes • TDMA and self-synchronization techniques are implemented in each node • lower data rates but higher communication range
Farr et al. [177, 178]	Acoustic + FSO	<ul style="list-style-type: none"> • high speed data transmission and sea floor monitoring system • used seafloor-based relay

on FSO using lasers limits the use-cases due to high-cost and form-factors of the experimentation platforms.

6 MAGNETIC INDUCTION BASED UNDERWATER COMMUNICATIONS

Another promising technology that is being studied recently is MI-based communication using induction rather than radiation, which reduces the impact of water conductivity. In the near field, the absorption loss caused by water conductivity is significantly reduced since the field does not propagate. If the desired communication range is d , we can choose the operating frequency to let $d/\lambda \ll 1$, where λ is the wavelength in water. Therefore, lower frequencies are used to obtain a long communication range using MI-based communication. Currently, the range of MI-based communication varies from several centimeters to hundreds of meters depending on the coil size, frequency, and transmission power. Note that, the major differences between the RF radiation-based communication and the MI-based communication are the distance and antenna. MI-based communication uses the near field and coil antenna.

This section proceeds as follows. We first introduce the main focus of this section that is different from existing surveys in Section 6.1. Then, we show the special signal propagation paths of MI-based communication signals in Section 6.2. After that, we present the networking technologies for underwater applications using MI-based communications 6.3. We also compare existing testbeds and the known communication performance in Section 6.4. We also provide an experimental measure study on underwater MI communication in Section 6.5. In the end, we discuss the open research problems and potential solutions in Section 6.6.

6.1 Existing Surveys

MI-based underwater communication channel models, antenna design, antenna array, system implementation, range and reliability improvement, and capacity enhancement have been surveyed in [6, 8, 179, 180]. Also, MI-based wireless communication is used in underground and related surveys provided in [181–184]. This section is different from existing surveys from the following aspects. First, most of existing surveys focus on deep underwater communication, while we pay attention to both shallow and deep underwater environments. In shallow underwater environment, the water surface changes the signal propagation path. Although reflections from the water surface can be easily modeled, the propagation of lateral wave is complex which demands special attention. Second, wireless underwater sensor networks using MI-based communication have not been fully established and there are limited works. In this section, we review the networking technologies

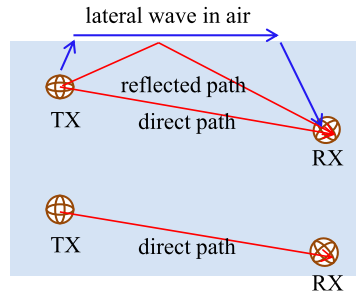


Fig. 7. Illustration of MI-based communication signal propagation paths in shallow underwater and deep underwater. In the deep underwater environment, the reflected path and the lateral wave are neglected.

using MI-based underwater communication. Third, there is a lack of comprehensive comparison of state-of-the-art empirical studies of MI-based underwater communication to understand the successful designs. In this section, we compare existing reported testbeds and results.

6.2 Underwater Signal Propagation for Magnetic Communication

Most of existing MI-based underwater communications consider a homogeneous underwater environment which is equivalent to the deep underwater environment where the impact of the water surface can be neglected. However, the water surface plays an important role in changing the signal propagation behavior in underwater. Here, we divide the MI-based underwater communication into two environments, namely the deep underwater and shallow underwater.

As shown in Figure 7, the deep underwater is dominated by the direct path. Since MI-based underwater communication using low frequency has a strong penetration efficiency, the scatters and reflectors in the vicinity of the transmitter and receiver can be neglected. The direct path channel is simple which is only determined by coil configurations, distance, and water dielectric parameters [6, 8, 179, 180]. In the shallow underwater environment, the MI-based communication signals propagate primarily in three paths, namely, the direct path, the reflected path, and the lateral wave in the air [185–187]. The lateral wave is due to the dielectric parameter difference between the air and the water. The relative permittivity of water is 81 times larger than that of the air. Also, considering the large conductivity of sea water, the difference of complex permittivity is also significant. The lateral wave propagates in the air which experiences less propagation loss. In this way, the communication range can be extended. However, as the depth increases, the MI-based communication signals attenuate significantly before they get to the water surface. As a result, the lateral wave becomes negligible. Only if the depths of the transmitter and receiver are much smaller than their distance, the lateral wave can play an important role. The rough water surface can also change the signal propagation significantly and analytical models are provided in [188].

The received signal power can be modeled using the following two models. First, in the deep underwater environment, the received signal power can be approximated by

$$P_r \approx \frac{P_t C_d}{r^6} e^{-2\alpha r} \quad (13)$$

where α is the attenuation factor which is given in (1), C_d is a constant that is determined by the configuration of coil antenna, r is the distance between the transmitter and the receiver, and P_t is the transmission power. It should be noted that when the signal carrier frequency is low and r is much smaller than the wavelength, the water conductivity can be neglected and the exponential

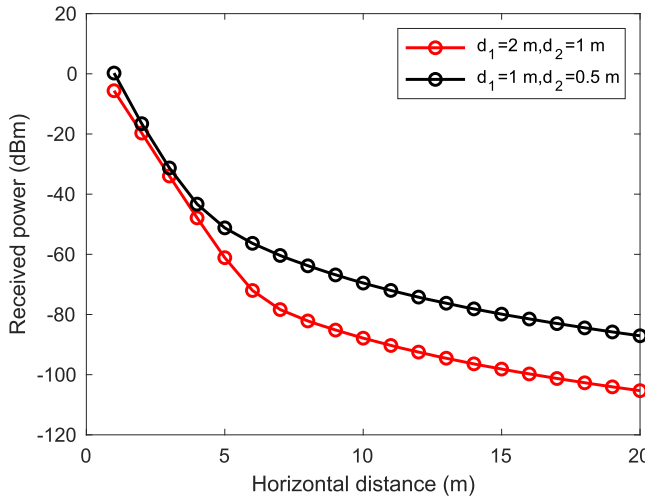


Fig. 8. Received power using tri-axis transceivers with a transmission power of 10 dBm. The transmitter and receiver depths are represented by d_1 and d_2 , respectively.

term can be considered as 1. The reflected path can be neglected since it has a longer distance than the direct path and therefore the signal attenuates much more significantly in lossy underwater environments. The shallow underwater channel is more complex mainly due to the lateral wave that propagates in the air and does not experience attenuation loss. To consider the impact of the lateral wave, the distance between the transmitter and the receiver should be much larger than the sum of their depths.

An example of the received power using tri-axis coil with the channel model in [189] is shown in Figure 8. The transmission power is 10 dBm. The depth of the transmitter (d_1) and receiver (d_2) are 2 m and 1 m, and 1 m and 0.5 m, respectively. The water conductivity is 0.5 S/m. The operating frequency is 1 MHz. The coil has a radius of 15 cm and number of turns of 10. As shown in the figure, in the first 5 m, the received power decreases very fast with more than 60 dB/decade. This is due to the attenuation loss in the water and the near field fast fall-off. As the distance increases, the lateral wave plays an important role and therefore the signal attenuates much slower.

6.3 Underwater Networking using Magnetic Induction Communications

Due to the limited communication range, underwater sensor networks using MI-based communication requires special networking technologies. In [4, 190], the magnetic waveguide is proposed to build a large scale underwater sensor network. Sensors are deployed in a periodic pattern, such as cubes, to maintain the efficiency of magnetic waveguide. Such a periodic structure can form a virtual wire that connects the source and destination. Although magnetic waveguide can extend the communication range, it requires scheduling and precise location of each sensor or passive relay, which is difficult to achieve in a dynamic underwater environment.

In [191], the MI-based underwater communication is used to synchronize underwater sensors or robots to coordinate their data transmission using acoustic communication. Underwater sensors and robots use short-range acoustic communications or MI-based communications to exchange information and coordinate their motion, while they use long-range acoustic communications with beamforming to send data to sinks that are far from them. The distributed MIMO system using acoustic communication requires precise synchronization among sensors or robots. Since the acoustic communication has a long delay and the channel experiences multipath fading which

is not reliable, MI-based underwater communication is used to send control and synchronization signals. In [189], the MI-based underwater communication is adopted for swarm robotics. Underwater robots use short-range communication to coordinate their motion to move towards their destinations. Their motion can ensure network connectivity.

6.4 Testbeds and Experiments

For kHz frequency band, a communication system using tri-axis coils is presented in [192]. The frequency is from 250 Hz to 10 kHz. The range is from 1 m to 5 m. It shows that using higher frequency, such as 10 kHz, can achieve longer range than that using 250 Hz. The high carrier frequency offers strong magnetic coupling. Due to the limitation of the hardware, i.e., MCC-DAQs' USB-3101FS data acquisition card and TI's TAS5630 300-W Class-D audio power amplifier (maximum frequency 10 kHz), carrier frequencies higher than 10 kHz are not discussed. The receiver uses a LT1167 low-noise amplifier. An interesting observation is that the noise level decreases as the frequency increases from 250 Hz to 10 kHz, which shows that in the underwater environment the noise is frequency dependent at such a low frequency band. The tri-axis coil's reliability is also tested and it is robust to angle misalignment.

In [193], high-sensitive wideband low-noise **anisotropic magnetoresistance (AMR)** magnetic field sensors are used as receivers. AMR sensors are widely used and can be easily adapted for MI-based communication. In [193], 100 kHz is used as the carrier frequency. By using small transmit (TX) coils with radius 1.6 cm, a communication range of 0.8 m can be obtained in real sea water.

In [194], a communication system using tri-axis coils and 125 kHz carrier frequency is presented. The ATA5276 transmitter and AS3933 receiver are employed to design the signal processing units. Results show that the MI-based communication can achieve low-power consumption, and the sensor node can survive as long as 28 years. The communication range measured in a swimming pool can be around 50 m.

A software-defined radio for MI-based communication is developed in [195]. The USRP X310 is used to obtain fully reconfigurable communication systems. The software implementation is performed in MATLAB. Although the coil size is comparable to the one in [194], due to the limited space in a water tank, the communication range is shorter. This paper developed a complete communication system and the achievable data rate is 24 kbps.

For MHz frequency band, [196] presents both in-lab and outdoor measurements. Matched loop antennas are used. It should be noted that sea water changes antenna impedance. Perfectly matched antenna in the air may not be matched in sea water. In-lab measurements are collected in a water tank where the transceivers are placed 1 m apart. A wide frequency range from 1 MHz to 66 MHz are used. Surprisingly, the difference of the received power of using 1 MHz and using 66 MHz is around 20 dBm, which is not significant considering the exponential loss in sea water. This shows that higher frequency may be used in sea water. More trials were undertaken in real sea water environment. The results show that the communication range can be longer than 50 m using 1 MHz carrier frequency in sea water. In [196], the near field loss and far field attenuation losses are compared, and it shows that the near field loss is much higher than the far field attenuation loss. In the far field, the major loss is the diffraction loss rather than the attenuation loss. In the near field, due to the proximity to the electrodes, conduction currents exist and the loss is higher, while in the far field the impact of the electrodes is small, the attenuation loss is negligible. The measurement in [197] also demonstrates a long communication range of 90 m using 5 MHz carrier frequency. The antenna is the same as the one used in [196]. Considering the shallow underwater environment, the lateral wave may play an important role in achieving the long communication range.

A prototype using off-the-shelf radios and microcontrollers is developed in [198]. The Freeline boards plus EMBware development boards are used as transceivers. Tri-axis coils with operating

Table 6. Summary of Existing Experimental MI-based Underwater Communication Systems

Ref.	Frequency	Coil size	Coil type	Range	Data rate	Environment
Ravindran et al. [192]	10 kHz	26 turns, 6.25 cm radius	tri-axis coil	5 m	10 kbps	sea water tank, coil depth 2.8 m
Ravindran et al. [192]	3 kHz	26 turns, 6.25 cm radius	tri-axis coil	10 m	1 kbps	sea water tank, coil depth 2.8 m
Al-Shamma`a et al. [196]	1 to 66 MHz	1 turn	loop antenna	1 m	-	sea water tank, coil depth 0.5 m to 1.5 m
Al-Shamma`a et al. [196]	1 MHz	1 turn	loop antenna	60 m	-	sea water, coil depth 2 to 3 m
Shaw et al. [197]	5 MHz	1 turn	loop antenna	90 m	500 kbps	sea water, coil depth 1.5 m
Hott et al. [193]	100 kHz	TX:10 turns, 1.6 cm radius	single coil	0.8 m	21.64 kbps	sea water
Ahmed et al. [194]	125 kHz	29 turns, 0.11 m radius	tri-axis coil	50 m	-	swimming pool
Wei et al. [195]	113 kHz	25 turns, 0.1 m radius	single coil	0.81 m	24 kbps	water tank
Gulati et al. [198]	13.56 MHz	9 turns, <0.025 m radius	tri-axis coil	2-3 m	-	water tank

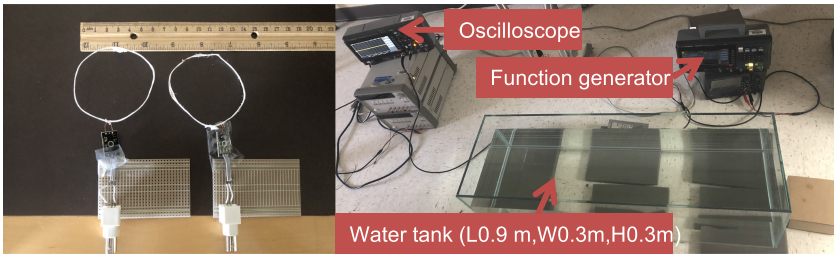


Fig. 9. Experimental setup using ANT-1356M coils and a water tank with dimension: length 0.9 m, width 0.3 m, and height 0.3 m.

frequency 13.56 MHz are adopted. The Freeline transmitter board is equipped with 3-axis magnetic coils; two of these three coils are wrapped around a ferrite-core whereas the third one is an air-core coil. The ferrite-core coils have a diameter of < 5 mm with 9 turns, whereas the air-core one is an ~46 mm × 66 mm rectangular coil. The Freeline receiver board is only equipped with an air-core rectangular coil. The transceivers were placed in a water tank to test the communication performance. With these coil dimensions, the authors have reported that the communication range in water is about 2 to 3 m.

Besides the above testbeds, there are also some other commercial products based on MI communication that can be used for wireless underwater communication such as [199, 200]. The detailed information of existing MI-based underwater communication testbeds are given in Table 6.

6.5 Understanding the Underwater MI Communication Characteristics through Measurements

We now show a proof-of-concept underwater MI communication system. We use ANT-1356M coil antennas, as shown in Figure 9. The coil has a diameter of 6.5 cm. The number of turns is 2. Also, the coil wire is not thick, and thus the coil shape is not a perfect circle. A water tank is used with dimension of length 0.9 m, width 0.3 m, and height 0.3 m, as shown in Figure 9. The tank is filled

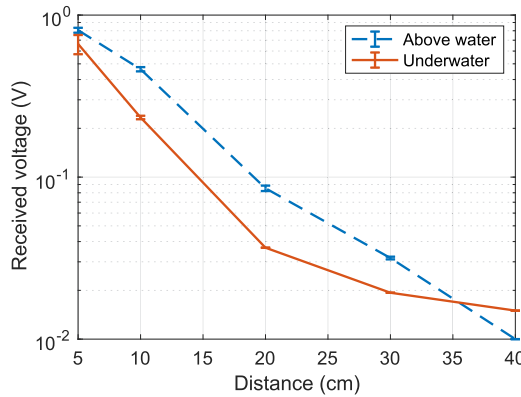


Fig. 10. Received voltage in the receiving coil. The above water and underwater are 5 cm above and under the water surface, respectively.

with normal tap water. The transmit coil is connected to a function generator with 10 Vpp sine output at 13.56 MHz and the receiver is connected to an oscilloscope to measure the peak-to-peak received voltages. First, we place both the transmit and receive coils above the water surface with a height of 5 cm. Then, we place both of them under the water surface with a depth of 5 cm. For each case, we measure three times and show the mean and variance in Figure 10. The measured range is 40 cm. Due to the small coil size and number of turns, the coupling between the two coils is weak. This can be improved by using larger coils with a higher number of turns. As we can see from Figure 10, the measurements at each distance have small variances which shows the high reliability of the MI communication channel. Also, the differences between the two cases is less than one order of magnitude, which shows that the water surface and water medium did not significantly attenuate magnetic signals.

6.6 Future Research Challenges

Although MI-based underwater communication has been extensively studied and we have a good understanding of the fundamental mechanism, there are still a few challenges unsolved or not effectively solved, such as the short communication range, low data rate, and so on.

6.6.1 Communication Ranges and Data Rates. MI-based underwater communication range is dependent on the coil configuration, carrier frequency, and transmission power. Most of underwater sensors and robots are battery-powered which have limited power and space. Reducing carrier frequency is effective in reducing propagation losses, but it also reduces the coupling between coils and the communication bandwidth. Thus, it is not trivial to obtain long-range MI-based underwater communications. For shallow underwater, due to the existence of lateral waves, the magnetic field propagation experiences less loss compared with the deep underwater case. We may leverage this property for long-range underwater applications. For deep underwater communication, acoustic communication is more suitable for long-range applications. Since MI-based underwater communication uses low frequency bands to obtain a reasonable communication range, the bandwidth is narrow. With a narrow bandwidth, it is challenging to achieve high-speed communication. To address this issue, advanced signal processing techniques can be leveraged, such as multiple-antenna systems and multicarrier modulations.

6.6.2 Hybrid System Design. There is no single technology that can achieve long-range, high-speed, and reliable underwater communications. Thus, the hybrid system will be a promising

Table 7. Comparison of Different Underwater Communication Technologies

Standard	RF	Acoustic	Optical	Magnetic
Frequency	1 Hz-2.485 GHz [205]	7-17 kHz [206] 27-31 kHz [208] 7.5-12 kHz [209]	430–790 THz	13.5 MHz [207] 3kHz, 10kHz [192]
Data rate	10 Mbps [202] 2400 kbaud [203] 100 bps [204] 150 kbps [203]	15 kbps [210] 6.9 kbps [206] 25-100 bps [208] 300 bps-2 kbps [209] 20-300 bps [213] 13.9 kbps [215]	1-5 Mbps [152] 2.5-10 Mbps [153] 500 Mbps [211] 80 kbps [212] 10 Mbps [214]	1 kbps - 10kbps [192] 24 kbps [195]
Range	2.5 cm [202] 1.5 m [203] 15-40 m [204] 2-10 m [203]	6 km [210] 8 km [206] 250 m [208] 20 km [209] 5-15 km [213] 3.5 km [215]	15 m [152] 150 m [153] 7 m [211] 1 m [212] 10-11 m [214]	2-3 m (@13.5 MHz) [198] 5-10m [192] 0.81 m [195]
Peak current/ power consumption	0.6 W [203] 16 W [204] 660 mA (@ 24 Vdc) [203]	3-45 W [206] 20 W [209] 75 W [213]	10–30 W [152] 10 W [153]	1.35 mA [200] 18 mA (FreeLinc) [207] 1.25 mW [195]

solution which leverages the advantages of existing solutions. For MI-based underwater communication, its major advantages compared with acoustic communication and optical communication include low delay, omni-directional propagation characteristics (compared with directional optical communication), and high penetration-efficiency in extreme environments. Although these properties have been well understood, it is still not clear in which situation we need to switch the communication mode to MI-based underwater communication. The fundamental analysis of a hybrid communication system, such as the RF and free-space optical communication in terrestrial environment [201], may provide guidelines to address this issue.

7 COMPARISON AND TRADEOFF BETWEEN DIFFERENT TECHNOLOGIES

7.1 Comparison of RF, Acoustic, Optical and MI Communications

In this section we compare the various communication technologies for UWSNs along with their pros and cons. The most mature technology is of course RF communication, however, the penetration decreases with increasing frequency. This makes lower frequency more attractive, however, the communication bandwidth decreases significantly. For example, by using modified off-the-shelf wireless Ethernet (802.11b) radios, the authors in [202] were able to achieve a transfer rate of 10 Mbps in sea water with a 2.5 cm antenna separation. The **Wireless for Subsea (WFS)** Seatooth S100 modem provides a datarate of 2400 kbaud with an operation range of 1.5 m through seawater [203]. Similarly S200 supports a datarate of 100 bps with a range of 15-40 m, whereas S300 provides a datarate of 156 kbps with a range of 2-10 m in seawater [204].

Acoustic signals are less affected in aqueous medium and are therefore more suitable for underwater communication than RF. Acoustic communication experiences low attenuation at low

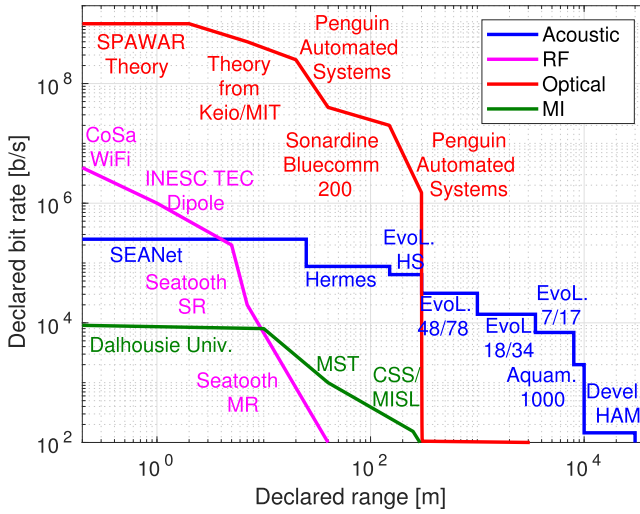


Fig. 11. Comparison between different communication technologies. Data taken from [106, 113].

frequencies, however, the achievable bandwidth will be lower at this frequency range. In addition, the speed of sound is also much less than electromagnetic signals, and therefore suffers from low propagation delay, multipath effects, and inter-symbol interference. All these severely limit the achievable data rate of acoustic communication. For example, Teledyne Benthos Underwater Acoustic Modems can transmit up to 15 kbps over a distance of 6 km in LF/MF band, and 2 km in C-band [210]. On the other hand, EvoLogics S2CR 7/17 modem supports a data rate up to 6.9 kbps over a range of 8 km [206], whereas S2CR 18/34 modem offers data transfer rates up to 13.9 kbps over a 3.5 km range [215]. AQUATEC AQUAmodem 500 offers a data rate of 25-100bps over a range of 250 m [208], whereas AQUAmodem 1000 offers 300 bps-2 kbps up to a range of 20 km [209]. MATS 3G underwater acoustic modem offers a data rate of 20-200 bps up to 15 km at 12 kHz, and 20-300 bps up to 5 km at 34 kHz [213]. The WHOI Micro-Modem operating at 900 Hz provides a data rate of few bits per second over a distance of 400 km [216]. HERMES is a high-speed, high-frequency acoustic modem that can transmit an uncompressed, high-resolution 400000 bit sonar image in 4.6 seconds, and can operate up to a range of 120 m [217].

Optical communication of 430–790 THz band has better penetration ability than RF and is suitable for ranges of few tens of meters. The technology can provide higher bandwidth as compared to RF, and has a lower propagation delay as compared to acoustics. The BlueComm 100 modem can achieve a data rate of 1-5 Mbps up to a range of 15 m [152]. On the other hand, BlueComm 200 offers a data rate of 2.5-10 Mbps up to a range of 150 m [153], whereas BlueComm 5000 achieves a data rate of 500 Mbps over a shorter distance up to 7 m [211]. Another commercial underwater optical modem is AQUAmodem Op2 which achieves a data rate of 80 kbps with a range of 1 m [212]. In [214] the authors have experimented with an optical modem that achieves a data rate of 10 Mbps over a distance of 10–11 m.

Magnetic induction or resonance-based communication range and data rate highly depends on the coil size, wire gauge, and number of turns. Also, fresh/lake water with low conductivity allow higher data rate and longer communication ranges than sea water. The communication range of most widely used magnetic coil with radius around 10 cm is about 10 m, such as [192]. The data rate ranges from 1 kbps to 100 kbps. Compared with the acoustic communication, MI communication has a short communication range, but it demonstrates low delay and a reliable channel. Compared

Table 8. Performance Figures of Some Representative Underwater Acoustic, Optical, Electromagnetic and Magneto-inductive Modems

	Manufacturer and model	Max Range	Bit rate
Acoustic	Develogics HAM.NODE [88]	30 km	145 bps
	AQUATEC AQUAmodem1000 [209]	10 km	{0.1, 2} kbps
	EvoLogics S2C R 7/17 [91]	7 km	{1, 7} kbps
	EvoLogics S2C R 18/34 [91]	3.5 km	{1, 13.9} kbps
	EvoLogics S2C R 48/78 [91]	1 km	{1, 32} kbps
	EvoLogics S2C M HS [91]	300 m	{2, 62} kbps
	FAU Hermes modem prototype [96]	150 m	87.7 kbps
	Rutgers MIMO modem [95]	10s of m	{100, 250} kbps
	Northeastern SEANet prototype [94]	10s of m	{41, 250} kbps
RF	CoSa WiFi [218]	10 cm	{10, 50} Mbps
	INESC TEC Dipole [219]	1 m	1 Mbps
	CoSa EF Dipole [218]	[1, 8] m	{0.2, 1} Mbps
	WFS Seetooth Mark IV SR [205]	[5, 7] m	2.4 kbps
	WFS Seetooth Mark IV MR [205]	[30, 45] m	100 bps
MI	Dalhousie Univ. Prototype [220]	10 m	8 kbps
	MST Prototype [194]	40 m	1 kbps
	CSS/MISL Prototype [221]	[250, 400] m	{153, 40} bps
Optical	Penguin Automated Systems [222]	[10, 300] m	{1.5, 100} Mbps
	Sonardyne BlueComm 200 [145]	120 m	10 Mbps
	MIT AquaOptical modem [147]	50 m	4 Mbps
	Hydromea Luma 500ER [223]	50 m	500 kbps

Data taken from [106, 113].

with the optical communication, MI communication has a low data rate, but it is robust in dirty water and omnidirectional in terms of directivity.

Table 7 summarizes the comparison of different wireless technologies for UWSNs. From the above analysis we can conclude that there is not a best technology for all working conditions; but given the application requirements in terms of datarate and range, there can be a technology that best suits those specific conditions. In general, multimodal communication systems where multiple transmission technologies are combined together, can provide significant benefits to the communication, as the system can switch the transmission device according to the observed channel conditions.

7.2 Suitability of the Wireless Technologies for Various Sensing Applications

In this section, we discuss the suitability of different wireless technologies in different underwater applications. Such an analysis can provide a guideline to the WSN community regarding specific usage of these technologies. Figure 11 and Table 8 summarize the tradeoff between data rate and communication range corresponding to different wireless technologies. As mentioned earlier, RF signals are badly absorbed in underwater medium; even if a reasonable level of range is achieved in VLF and ELF bands, the datarate falls short to make it applicable in any realistic scenario.

Acoustic and optical/VLC communication are suitable for long distance underwater applications. Acoustic communication works well up to several kilometers in lower frequency bands; however the datarate remains quite low (i.e., 20 bps to 15 kbps). At the same time the power consumption for acoustic communication is also high. Therefore, the technology can be useful for

low datarate applications, such as continuous monitoring scenarios (i.e., marine life monitoring or climate monitoring applications). However, the technology is not well suited for applications that require video/audio information, such as underwater disaster monitoring applications that occasionally require video transmissions. On the other hand, optical communication technologies also provide descent transmission range (i.e., 10–150 m). Although this range is lower as compared to acoustic, the optical technology can support significantly higher datarate (i.e., 1–100 Mbps). Therefore, optical transceivers can be very well suited for high datarate underwater communication (i.e., video).

MI communication demonstrates shorter transmission range as compared to acoustic and optics; however the power consumption typically remains small. Although the range can be extended by using low frequency and larger coils; the transmission range cannot be extended more than few tens of meters. Therefore, this technology is suitable for habitat monitoring applications (i.e., fisheries management) within a confined or targeted region. Also, as the technology consumes very low power, this is suitable for prolonged monitoring applications.

The above analysis provide some key insights to the sensor network community and engineers about the suitability of various technologies for different underwater applications. Along with that the engineers can also get crucial insights about the sensor deployment strategies, along with their numbers and densities, depending on the applications and chosen technology. For example, in the case of acoustic and optical communication, the range is quite high; therefore a sparse deployment is sufficient, whereas in the case of MI communication the range is quite limited, which requires dense sensor deployment.

7.3 Possibilities of Multimodal Underwater Networks

As mentioned earlier, different wireless technologies have their respective advantages and limitations; therefore a promising line of research is to explore the feasibility of multimodal communication systems. A multimodal system [113] is able to optimally select the best performing technology to establish a communication link between two nodes in certain channel conditions and can provide significant benefits. In addition, the MAC [105] and routing [104] layer protocols need to be designed taking into account the availability of different technologies, while achieving a higher network throughput and a lower end-to-end packet delivery delay than the ones that can be obtained with single technology underwater networks. Several applications can be enabled by such a system. For example, in [224–226] authors proved how the use of acoustic and optical communication in a scenario where an AUV patrols an area to collect data from submerged sensors can use acoustics to identify the nodes' position, and switch to optical communication as soon as it approaches the nodes to download a large amount of data in a very short amount of time (Figure 12(a)), reducing the time and the power consumption required to download the data via single mode acoustic communication. In the framework of multimodal network, we can consider not only networks with different communication technologies, but also networks that use different types of modems with different frequencies. For instance, in [99] the authors proved that an underwater acoustic network equipped with both low rate medium frequency low cost acoustic modems and sophisticated high rate high frequency acoustic modems can entail a significant improvement in the overall network throughput in a data muling scenario. In addition, the whole EDA SALSA [93] project is base on an adaptive acoustic network, whose nodes can decide to switch not only between different communication modulation and coding schemes, but also between LF and HF acoustic modems.

Another application that has been widely inspected by many research institutes and offshore companies is the possibility to deploy a wireless remotely controlled ROV [106, 227, 228] (Figure 12(b)). Both simulation and field tests proved that optical communication can provide,

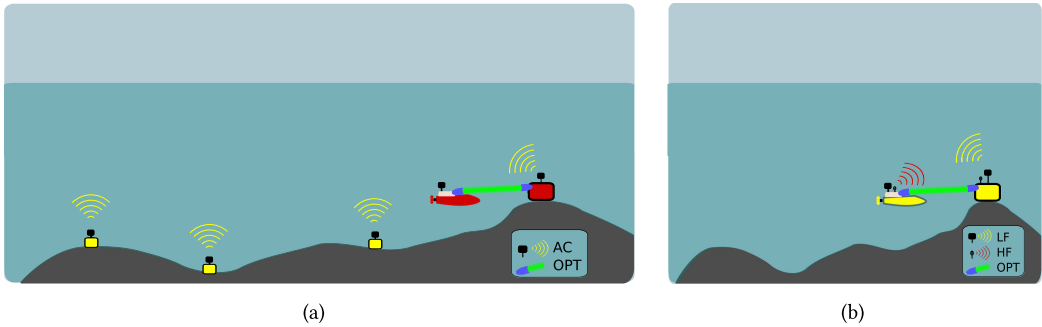


Fig. 12. Most representative applications of underwater multimodal networks: data retrieval from submerged sensors (a) and remote control for underwater vehicles (b). In this figure, AC and OPT denote acoustic and optical communication respectively, whereas LF and HF denote low-frequency and high-frequency acoustic communication respectively.

when in range, a datarate high enough to pilot the ROV with performance akin to the one experienced with the umbilical cable, however an acoustic backup link must be used to keep the connection between control station and vehicle in case the optical link gets disrupted due to, for instance, the presence of obstacles that interrupt the line of sight. In this scenario, in [106] the authors considered both the use of HF and LF acoustic modems, in order to be able to still convey high quality images via acoustic HF when the optical modem is out of range and the distance between ROV and control station is less than 300 m, and keep only information on the ROV status when the vehicle is moving in an area far away from the control station, performing an autonomous mission, and hence behaving like an AUV. This behavior is typical of resident ROVs deployed in oil and gas fields, that often travel for a few kilometers in an autonomous way before reaching the area of interest for the pipeline inspection.

An interesting aspect when talking about multimodal network is deciding when to switch between one technology to another. Reactive [229] and proactive [226] approaches have been investigated by researchers. The former requires the probe of all available channels every time a link gets disrupted to select the best performing one in range; the latter performs a prediction based on the received signal of which available channel will provide the best performance, trying to estimate the quality of all channels available from the observations performed to only one of them (e.g., the last one observed, i.e., the channel currently used for the communication) [72]. While a reactive approach ensures selecting the best channel available in that precise moment, a proactive approach allows for foreseen channel disruption and limits their effect by switching channels before any disruption occurs. In the last five years many multimodal architectures have been presented by different research institutes [114, 218, 224–226, 230], indicating a substantial amount of research possibilities in this direction.

8 CONCLUSION

Like terrestrial wireless sensor networks, UWSNs find various applications that require both continuous (i.e., marine habitat or climate monitoring) as well as event driven monitoring (i.e., underwater pipeline or disaster monitoring). However, as opposed to the above-ground, terrestrial communication, exploring robust communication is quite challenging in marine environments due to the high conductivity of the water medium, along with other underwater factors like attenuation, reflection, scattering, multipath effects, and so on. This paper provides a comprehensive study of various facets of underwater propagation, along with the strengths and

limitations of underwater wireless communication technologies. To be more specific, this article summarizes four different communication technologies for UWSNs, namely radio communication, acoustics, magnetic, and VLC. Among these technologies, the radio communication experiences high signal absorption, whereas acoustics provides long-range communication with long signal delay. Magnetic and VLC appears as the other two promising technologies for providing high data rate underwater communication. The article also demonstrates various underwater propagation characteristics on these technologies through detailed experimental studies. Through detailed comparison, we can conclude that no single technology can offer a win-win outcome in all environments, which stems the motivation for designing multimodel solutions. We hope that such a well-structured research summary will spur researchers to further examine and overcome the communication issues for reliable UWSNs.

REFERENCES

- [1] Ian F. Akyildiz, Pu Wang, and Zhi Sun. 2015. Realizing underwater communication through magnetic induction. *IEEE Communications Magazine* 53, 11 (2015), 42–48.
- [2] X. Che, I. Wells, G. Dickers, P. Kear, and X. Gong. 2010. Re-evaluation of RF electromagnetic communication in underwater sensor networks. *IEEE Communications Magazine* 48, 12 (2010), 143–151.
- [3] Liu Lanbo, Zhou Shengli, and Cui Jun-Hong. 2008. Prospects and problems of wireless communication for underwater sensor networks. *Wireless Communications and Mobile Computing* 8, 8 (2008), 977–994.
- [4] M. C. Domingo. 2012. Magnetic induction for underwater wireless communication networks. *IEEE Transactions on Antennas and Propagation* 60, 6 (June 2012), 2929–2939. DOI: <http://dx.doi.org/10.1109/TAP.2012.2194670>
- [5] Hassan M. Oubei, Chao Shen, Abla Kammoun, Emna Zedini, Ki-Hong Park, Xiaobin Sun, Guangyu Liu, Chun Hong Kang, Tien Khee Ng, Mohamed-Slim Alouini, and Boon S. Ooi. 2018. Light based underwater wireless communications. *Japanese Journal of Applied Physics* 57, 8S2 (2018).
- [6] Mohammed Jouhari, Khalil Ibrahim, Hamidou Tembine, and Jalel Ben-Othman. 2019. Underwater wireless sensor networks: A survey on enabling technologies, localization protocols, and internet of underwater things. *IEEE Access* 7 (2019), 96879–96899.
- [7] Camila Gussen, Paulo Diniz, Marcello Campos, Wallace Martins, Felipe Costa, and Jonathan Gois. 2016. A survey of underwater wireless communication technologies. *Journal of Communication and Information Systems* 31 (1 2016), 242–255.
- [8] Yuzhou Li, Shengnan Wang, Cheng Jin, Yu Zhang, and Tao Jiang. 2019. A survey of underwater magnetic induction communications: Fundamental issues, recent advances, and challenges. *IEEE Communications Surveys & Tutorials* 21, 3 (2019), 2466–2487.
- [9] Nasir Saeed, Abdulkadir Celik, Tareq Y. Al-Naffouri, and Mohamed-Slim Alouini. 2019. Underwater optical wireless communications, networking, and localization: A survey. *Ad Hoc Networks* 94 (2019), 101935.
- [10] Mohsin Murad, Adil A. Sheikh, Muhammad Asif Manzoor, Emad Felemban, and Saad Qaisar. 2015. A survey on current underwater acoustic sensor network applications. *International Journal of Computer Theory and Engineering* 7, 1 (2015), 51.
- [11] Emma V. Sheehan, Stephen C. Votier, Anthony W. J. Bicknell, Brendan J. Godley, and Matthew J. Witt. 2016. Camera technology for monitoring marine biodiversity and human impact. *Frontiers in Ecology and the Environment* 14, 8 (2016), 424–432.
- [12] Stefan B. Williams, Oscar Pizarro, Michael V. Jakuba, Craig R. Johnson, Neville Barrett, Russell C. Babcock, Gary A. Kendrick, Peter D. Steinberg, Andrew J. Heyward, Peter J. Doherty, Ian Mahon, Matthew Johnson-Roberson, Daniel M. Steinberg, and Ariell Friedman. 2012. Monitoring of benthic reference sites: Using an autonomous underwater vehicle. *IEEE Robotics Autom. Mag.* 19, 1 (2012), 73–84.
- [13] Karen Anderson and Kevin J. Gaston. 2013. Lightweight unmanned aerial vehicles will revolutionize spatial ecology. *Frontiers in Ecology and the Environment* 11, 3 (2013), 138–146.
- [14] G. Açar. 2006. ACMENet: An underwater acoustic sensor network protocol for real-time environmental monitoring in coastal areas. *IEE Proceedings - Radar, Sonar and Navigation* 153 (2006), 365–380. Issue 4.
- [15] Acoustic communication network for monitoring of underwater environment in coastal areas (ACME). <https://cordis.europa.eu/project/id/EVK3-CT-2000-00039/es>. ([n. d.]).
- [16] Long Range Telemetry in Ultra-Shallow Channels. <https://cordis.europa.eu/project/id/MAS3970099>. ([n. d.]).
- [17] Hong Kwang Yeo, B. S. Sharif, A. E. Adams, and O. R. Hinton. 2001. Performances of multi-element multi-user detection strategies in a shallow-water acoustic network (SWAN). *IEEE Journal of Oceanic Engineering* 26, 4 (2001), 604–611.

- [18] CoralSense. <https://sites.google.com/site/uwsnuqu/>. ([n. d.]).
- [19] Matt Bromage, Katia Obraczka, and Donald Potts. 2007. SEA-LABS: A wireless sensor network for sustained monitoring of coral reefs. In *Networking*, Vol. 4479. 1132–1135.
- [20] Gordon D. Hastie, Gi-Mick Wu, Simon Moss, Pauline Jepp, Jamie MacAulay, Arthur Lee, Carol E. Sparling, Clair Evers, and Douglas Gillespie. 2019. Automated detection and tracking of marine mammals: A novel sonar tool for monitoring effects of marine industry. 29, S1 (2019), 119–130.
- [21] Sarah J. Nancollas, Simon J. Pittman, Emma V. Sheehan, and Danielle Bridger. 2020. PelagiCam: A novel underwater imaging system with computer vision for semi-automated monitoring of mobile marine fauna at offshore structures. *Environ. Monit. Assess* 192, 11 (2020), 1–13.
- [22] Underwater Monitoring for Oil & Gas Market to Cross \$1.8 Billion by 2024. <https://www.techsciresearch.com/news/4420-underwater-monitoring-for-oil-gas-market-to-cross-1-8-billion-by-2024.html>. ([n. d.]). Last time accessed: Feb. 2021.
- [23] Underwater Monitoring System for Oil & Gas Market Anticipated to Reach US\$ 1,181.3 Mn by 2025: Transparency Market Research. <https://www.prnewswire.com/news-releases/underwater-monitoring-system-for-oil-gas-market-anticipated-to-reach-us-11813-mn-by-2025-transparency-market-research-642117893.html>. ([n. d.]). Last time accessed: Feb. 2021.
- [24] B. Thornton, A. Bodenmann, A. Asada, T. Sato, and T. Ura. 2012. Acoustic and visual instrumentation for survey of manganese crusts using an underwater vehicle. In *OCEANS*. 1–10.
- [25] S. Srinivas, P. Ranjitha, R. Ramya, and G. K. Narendra. 2012. Investigation of oceanic environment using large-scale UWSN and UANETs. In *WiCOM*. 1–5.
- [26] A. Vasilijević, Đ. Nađ, F. Mandić, N. Mišković, and Z. Vukić. 2017. Coordinated navigation of surface and underwater marine robotic vehicles for ocean sampling and environmental monitoring. *IEEE/ASME Transactions on Mechatronics* 22, 3 (2017), 1174–1184.
- [27] Leif Solberg and Gjertveit Erling. 2007. Constructing the world’s longest subsea pipeline, Langedag gas export. In *Offshore Technology Conference*.
- [28] Stewart William Behie, Robert Fryer, Mike Ashby, Hassan Al Emadi, Ali Al Rahbi, and Larry Laczko. 2008. Managing risks during the transition of Dolphin energy project from construction to full operations. In *SPE Middle East Health, Safety, Security, and Environment Conference and Exhibition*.
- [29] Underwater Pipeline Damage Underestimated in Gulf. <https://www.npr.org/templates/story/story.php?storyId=5383631?storyId=5383631>. ([n. d.]). Last time accessed: March 2021.
- [30] Pipelines Explained: How Safe are America’s 2.5 Million Miles of Pipelines? <https://www.propublica.org/article/pipelines-explained-how-safe-are-americas-2-5-million-miles-of-pipelines>. ([n. d.]). Last time accessed: Feb. 2021.
- [31] Nader Mohamed, Imad Jawhar, Jameela Al-Jaroodi, and Liren Zhang. 2011. Sensor network architectures for monitoring underwater pipelines. *Sensors* 11 (2011), 10738–10764.
- [32] N. Mohamed, I. Jawhar, J. Al-Jaroodi, and L. Zhang. 2010. Monitoring underwater pipelines using sensor networks. In *IEEE HPCC*. 346–353.
- [33] Huda Aldosari, Raafat S. Elfouly, Reda Ammar, and Mohammad Alsulami. 2020. New monitoring architectures for underwater oil/gas pipeline using hyper sensors. In *CATA (EPIc Series in Computing)*, Vol. 69. 307–316.
- [34] A New Tsunami-Warning System. <https://www.who.edu/oceanus/feature/a-new-tsunami-warning-system/>. ([n. d.]). Last time accessed: Feb. 2021.
- [35] Real-Time Seismic Monitor Installed on Growing Underwater Volcano. https://www.nsf.gov/news/news_summ.jsp?cntn_id=108985. ([n. d.]). Last time accessed: Feb. 2021.
- [36] M. Purcell, D. Gallo, G. Packard, M. Dennett, M. Rothenbeck, A. Sherrell, and S. Pascaud. 2011. Use of REMUS 6000 AUVs in the search for the Air France Flight 447. In *OCEANS*. 1–7.
- [37] Argo project. <https://argo.ucsd.edu/about/>. ([n. d.]). Last time accessed: Feb. 2021.
- [38] A. Palmeiro, M. Martini, I. Crowther, and M. Rhodes. 2011. Underwater radio frequency communications. In *OCEANS*. 1–8.
- [39] Arsen Zoksimovski, Daniel Sexton, Milica Stojanovic, and Carey M. Rappaport. 2015. Underwater electromagnetic communications using conduction - channel characterization. *Ad Hoc Networks* 34 (2015), 42–51.
- [40] Michael R. Frater, Michael J. Ryan, and Robin M. Dunbar. 2006. Electromagnetic communications within swarms of autonomous underwater vehicles. In *WUWNET*, Jun-Hong Cui, Urbashi Mitra, Kevin R. Fall, and Milica Stojanovic (Eds.). 64–70.
- [41] Shan Jiang and Stavros Georgakopoulos. 2011. Electromagnetic wave propagation into fresh water. *Journal of Electromagnetic Analysis and Applications* 3, 7 (2011), 261–266.
- [42] M. Callahan. 1981. Submarine communications. *IEEE Communications Magazine* 19, 6 (1981), 16–25.
- [43] Igor Smolyaninov, Quirino Balzano, and Dendy Young. 2020. Development of broadband underwater radio communication for application in unmanned underwater vehicles. *Journal of Marine Science and Engineering* 8, 5 (2020).

- [44] S. Sendra, J. V. Lamparero, J. Lloret, and M. Ardid. 2011. Underwater communications in wireless sensor networks using WLAN at 2.4 GHz. In *IEEE MASS*. 892–897.
- [45] Jaime Lloret, Sandra Sendra, Miguel Ardid, and Joel J. P. C. Rodrigues. 2012. Underwater wireless sensor communications in the 2.4 GHz ISM frequency band. *Sensors* 12, 4 (2012), 4237–4264.
- [46] Reiner Jedermann, Thomas Pötsch, and Chanaka Lloyd. 2014. Communication techniques and challenges for wireless food quality monitoring. *Philosophical Transactions of the Royal Society of London A: Mathematical, Physical and Engineering Sciences* 372, 2017 (2014), 20130304.
- [47] Faisal Ali Khan. 2015. *Sub-Gigahertz Wireless Sensors for Monitoring of Food Transportation*. Master’s thesis. University Bremen.
- [48] M. Siegel and R. King. 1973. Electromagnetic propagation between antennas submerged in the ocean. *IEEE Transactions on Antennas and Propagation* 21, 4 (1973), 507–513.
- [49] Extremely Low Frequency Transmitter Site Clam Lake, Wisconsin. https://fas.org/nuke/guide/usa/c3i/fs_clam_lake_elf2003.pdf. ([n. d.]). Last time accessed: Feb. 2021.
- [50] Shan Jiang. 2011. Electromagnetic wave propagation into fresh water. *Journal of Electromagnetic Analysis and Application* 3 (2011), 261–266.
- [51] Marco Lanzagorta. 2012. *Underwater Communications*. Vol. 5.
- [52] R. K. Moore. 1967. Radio communication in the sea. *IEEE Spectrum* 4, 11 (1967), 42–51.
- [53] H. Rowe. 1974. Extremely low frequency (ELF) communication to submarines. *IEEE Transactions on Communications* 22, 4 (1974), 371–385.
- [54] H. B. Singh and Rajendra Pal. 2013. Submarine communications. *Defence Science Journal* 43, 1 (2013), 43–51.
- [55] Deep secret – secure submarine communication on a quantum level. <https://www.naval-technology.com/features/featuredeep-secret-secure-submarine-communication-on-a-quantum-level/>. ([n. d.]). Last time accessed: Feb. 2021.
- [56] Milica Stojanovic and James C. Preisig. 2009. Underwater acoustic communication channels: Propagation models and statistical characterization. *IEEE Communications Magazine* 47, 1 (2009), 84–89.
- [57] M. Stojanovic. 1995. Underwater acoustic communications. In *IEEE Electro International*. 435–440.
- [58] G. Lee, J. Lee, T. Kang, K. Kim, and W. Kim. 2019. Experimental results of long range underwater communication based on chirp-FH signals. In *ICUFN*. 39–41.
- [59] Francisco Cañete, Jesús López-Fernández, Celia García-Corrales, Antonio Sánchez, Encarnación Robles, Francisco Rodrigo, and José Paris. 2016. Measurement and modeling of narrowband channels for ultrasonic underwater communications. *Sensors* 16, 2 (2016), 256.
- [60] M. Stojanovic. 2007. On the relationship between capacity and distance in an underwater acoustic communication channel. *ACM Mobile Comput. and Commun. Review* 11, 4 (Oct. 2007), 34–43.
- [61] R. Thiele and G. Schellstede. 1980. *Standardwerte zur Ausbreitungsdämpfung in der Nordsee*. Technical Report. Die Forschungsanstalt der Bundeswehr für Wasserschall und Geophysik (FWG), Kiel, Deutschland.
- [62] Mandar Chitre. 2006. *Underwater Acoustic Communications in Warm Shallow Water Channels*. (2006). PhD Thesis, National University of Singapore, Singapore.
- [63] Robert J. Urick. 1983. *Principles of Underwater Sound* (3rd ed.).
- [64] Leif Abrahamsson. 2003. *RAYLAB - A Ray Tracing Program in Underwater Acoustics*. Technical Report. Swedish Defence Research Agency (FOI), Stockholm, Sweden.
- [65] Frank Gerdes, Hans-Günter Hofmann, Wolfgang Jans, Steffen Künzel, Ivor Nissen, and Henry Dol. 2009. Measurements and simulations of acoustic propagation loss in the Baltic Sea. In *Underwater Acoustic Measurements*. Nafplion, Greece.
- [66] M. Porter et al. Bellhop code. ([n. d.]). <http://oalib.hlsresearch.com/Rays/index.html>. Last time accessed: Jan. 2014.
- [67] Michael Zuba, Zaihan Jiang, T. C. Yang, Yishan Su, and J. Cui. 2013. An advanced channel framework for improved underwater acoustic network simulations. In *Proc. IEEE/MTS OCEANS*. San Diego, CA.
- [68] A. Mahmood, M. Chitre, and H. Vishnu. 2017. Locally optimal inspired detection in snapping shrimp noise. *IEEE Journal of Oceanic Engineering* 42, 4 (2017), 1049–1062. DOI: <http://dx.doi.org/10.1109/JOE.2017.2731058>
- [69] Emanuele Coccolo, Filippo Campagnaro, Alberto Signori, Federico Favaro, and Michele Zorzi. 2018. Implementation of AUV and ship noise for link quality evaluation in the DESERT underwater framework. In *Proc. ACM WUWNet, Shenzhen, China*.
- [70] R. Chen, A. Poulsen, and H. Schmidt. 2019. Spectral, spatial, and temporal characteristics of underwater ambient noise in the Beaufort Sea in 1994 and 2016. *Journal of the Acoustical Society of America* 145, 605 (Feb. 2019), 605–614. DOI: <http://dx.doi.org/10.1121/1.5088601>
- [71] Noise Field in the Arctic. <https://dosits.org/science/sounds-in-the-sea/noise-field-in-the-arctic/>. ([n. d.]). Last time accessed: Feb. 2021.
- [72] R. Diamant, F. Campagnaro, M. de Filippo de Grazia, P. Casari, A. Testolin, V. Sanjuan Calzado, and M. Zorzi. 2017. On the relationship between the underwater acoustic and optical channels. *IEEE Transactions on Wireless Communications* 16, 12 (2017), 8037–8051. DOI: <http://dx.doi.org/10.1109/TWC.2017.2756055>

- [73] P. H. Rogers. 1981. *Onboard Prediction of Propagation Loss in Shallow Water*. Naval Research Lab Defense Technical Information Center, Washington, DC.
- [74] F. Campagnaro, R. Francescon, F. Guerra, F. Favaro, P. Casari, R. Diamant, and M. Zorzi. 2016. The DESERT underwater framework v2: Improved capabilities and extension tools. In *2016 IEEE Third Underwater Communications and Networking Conference (UComms)*. 1–5. DOI: <http://dx.doi.org/10.1109/UComms.2016.7583420>
- [75] ns3 UAN Framework. ([n. d.]). <https://www.nsnam.org/docs/release/3.12/models/html/uan.html>. Last time accessed: Jan. 2014.
- [76] Paolo Casari, Filippo Campagnaro, Elizaveta Dubrovinskaya, Roberto Francescon, Amir Dagan, Shlomo Dahan, Michele Zorzi, and Roei Diamant. 2020. ASUNA: A topology dataset for underwater network emulation. *IEEE Journal of Oceanic Engineering* (March 2020). Early Access.
- [77] H. Maulana, M. A. Prihandono, A. S. Elfa, R. Harwahyu, and R. F. Sari. 2019. Analysis of VBF and DBR performance in environmental monitoring system using Aquasim at NS-3. In *2019 International Conference on Informatics, Multimedia, Cyber and Information System (ICIMCIS)*. 17–22. DOI: <http://dx.doi.org/10.1109/ICIMCIS48181.2019.8985348>
- [78] F. Guerra, P. Casari, and M. Zorzi. 2009. World ocean simulation system (WOSS): A simulation tool for underwater networks with realistic propagation modeling. In *Proc. of ACM WUWNet 2009*. Berkeley, CA.
- [79] R. Petroccia and D. Spaccini. 2013. A back-seat driver for remote control of experiments in underwater acoustic sensor networks. In *2013 MTS/IEEE OCEANS - Bergen*. 1–9. DOI: <http://dx.doi.org/10.1109/OCEANS-Bergen.2013.6608129>
- [80] M. Chitre, R. Bhatnagar, and W. Soh. 2014. UnetStack: An agent-based software stack and simulator for underwater networks. In *2014 OCEANS - St. John's*. 1–10. DOI: <http://dx.doi.org/10.1109/OCEANS.2014.7003044>
- [81] J. Alves, J. Potter, P. Guerrini, G. Zappa, and K. LePage. 2014. The LOON in 2014: Test bed description. In *2014 Underwater Communications and Networking (UComms)*. 1–4. DOI: <http://dx.doi.org/10.1109/UComms.2014.7017141>
- [82] SUNRISE Testbed Federation. ([n. d.]). <http://fp7-sunrise.eu/index.php/testbed-federation/description>. Last time accessed: Jan. 2014.
- [83] M. Molins and M. Stojanovic. 2006. Slotted FAMA: A MAC protocol for underwater acoustic networks. In *OCEANS 2006 - Asia Pacific*. 1–7. DOI: <http://dx.doi.org/10.1109/OCEANSAP.2006.4393832>
- [84] S. Lmai, M. Chitre, C. Laot, and S. Houcke. 2017. Throughput-efficient super-TDMA MAC transmission schedules in ad hoc linear underwater acoustic networks. *IEEE Journal of Oceanic Engineering* 42, 1 (2017), 156–174. DOI: <http://dx.doi.org/10.1109/JOE.2016.2537659>
- [85] R. Diamant, P. Casari, F. Campagnaro, and M. Zorzi. 2017. Leveraging the near–far effect for improved spatial-reuse scheduling in underwater acoustic networks. *IEEE Transactions on Wireless Communications* 16, 3 (2017), 1480–1493. DOI: <http://dx.doi.org/10.1109/TWC.2016.2646682>
- [86] M. Goetz and I. Nissen. 2012. GUWMANET - multicast routing in underwater acoustic networks. In *IEEE 2012 Military Communications and Information Systems Conference (MCC)*.
- [87] A. Issac, S. A. Samad, and A. S. Jereesh. 2017. Software tools for simulation and realization of underwater networks. In *2017 International Conference on Communication and Signal Processing (ICCSP)*. 457–461. DOI: <http://dx.doi.org/10.1109/ICCSP.2017.8286399>
- [88] Develogic Subsea Systems. <http://www.develogic.de/>. ([n. d.]). Last time accessed: Feb. 2021.
- [89] Cristiano Tapparello, Paolo Casari, Giovanni Toso, Ivano Calabrese, Roald Otnes, Paul van Walree, Michael Goetz, Ivor Nissen, and Michele Zorzi. 2013. Performance evaluation of forwarding protocols for the RACUN network. In *Proc. ACM WUWNet*, Kaohsiung, Taiwan.
- [90] J. Potter, J. Alves, D. Green, G. Zappa, I. Nissen, and K. McCoy. 2014. The JANUS underwater communications standard. In *Proc. UComms*, Sestri Levante, Italy.
- [91] EvoLogics 18/34 communication and positioning devices. ([n. d.]). <https://evologics.de/acoustic-modems>. Last time accessed: Feb. 2021.
- [92] Vladimir Djapic, Wenjie Dong, Daniele Spaccini, Gianni Cario, Alessandro Casavola, Petrika Gjanci, Marco Lupia, and Chiara Petrioli. 2016. Cooperation of coordinated teams of autonomous underwater vehicles. *9th IFAC Symposium on Intelligent Autonomous Vehicles LAV* 49, 15 (July 2016), 88–93.
- [93] H. Dol. 2019. EDA-SALSA: Towards smart adaptive underwater acoustic networking. In *OCEANS 2019 - Marseille*. 1–6. DOI: <http://dx.doi.org/10.1109/OCEANSE.2019.8867361>
- [94] Emrecan Demirors, Bharatwaj G. Shankar, G. Enrico Santagati, and Tommaso Melodia. 2015. SEANet: A software-defined acoustic networking framework for reconfigurable underwater networking. In *Proc. ACM WUWNet*, Washington DC, US.
- [95] M. Rahmati, A. Gurney, and D. Pompili. 2018. Adaptive underwater video transmission via software-defined MIMO acoustic modems. In *Proc. MTS/IEEE OCEANS*, Charleston.
- [96] Pierre-Philippe Beaujean, John Spruance, E. A. Carlson, and D. Kriel. 2008. HERMES - a high-speed acoustic modem for real-time transmission of uncompressed image and status transmission in port environment and very shallow water. In *Proc. MTS/IEEE OCEANS*, Québec City, Canada.

- [97] Water Linked M64 Acoustic Modem. <https://bluerobotics.com/store/comm-control-power/acoustic-modems/wl-11003-1/>. ([n. d.]). Last time accessed: Feb. 2021.
- [98] Christian Renner and Alexander J. Golkowski. 2016. Acoustic modem for micro AUVs: Design and practical evaluation. In *Proceedings of the Eleventh ACM International Workshop on Underwater Networks (WUWNet'16)*. Shanghai, China.
- [99] Alberto Signori, Filippo Campagnaro, Fabian Steinmetz, Bernd-Christian Renner, and Michele Zorzi. 2019. Data gathering from a multimodal dense underwater acoustic sensor network deployed in shallow fresh water scenarios. *MDPI Journal of Sensor and Actuator Networks* 8, 4 (2019), 55.
- [100] Alberto Signori, Federico Chiariotti, Filippo Campagnaro, and Michele Zorzi. 2020. A game-theoretic and experimental analysis of energy-depleting underwater jamming attacks. *IEEE Internet of Things Journal* 7, 10 (Oct. 2020), 9793–9804.
- [101] B. Tomasi, P. Casari, L. Finesso, G. Zappa, K. McCoy, and M. Zorzi. 2010. On modeling JANUS packet errors over a shallow water acoustic channel using Markov and hidden Markov models. In *2010 - MILCOM 2010 Military Communications Conference*. 2406–2411. DOI: <http://dx.doi.org/10.1109/MILCOM.2010.5680327>
- [102] Beatrice Tomasi, Paolo Casari, Leonardo Badia, and Michele Zorzi. 2015. Cross-layer analysis via Markov models of incremental redundancy hybrid ARQ over underwater acoustic channels. *Ad Hoc Networks* 34 (2015), 62–74. DOI: <http://dx.doi.org/10.1016/j.adhoc.2014.07.013> *Advances in Underwater Communications and Networks*.
- [103] M. Goetz, I. Nissen, R. Otnes, and P. van Walree. 2015. Performance analysis of underwater network protocols within international sea trial. In *OCEANS 2015 - Genova*. 1–7. DOI: <http://dx.doi.org/10.1109/OCEANS-Genova.2015.7271400>
- [104] R. Diamant, P. Casari, F. Campagnaro, O. Kebkal, V. Kebkal, and M. Zorzi. 2018. Fair and throughput-optimal routing in multimodal underwater networks. *IEEE Transactions on Wireless Communications* 17, 3 (2018), 1738–1754. DOI: <http://dx.doi.org/10.1109/TWC.2017.2785223>
- [105] F. Campagnaro, P. Casari, M. Zorzi, and R. Diamant. 2019. Optimal transmission scheduling in small multimodal underwater networks. *IEEE Wireless Communications Letters* 8, 2 (2019), 368–371. DOI: <http://dx.doi.org/10.1109/LWC.2018.2873329>
- [106] Filippo Campagnaro, Alberto Signori, and Michele Zorzi. 2019. Wireless remote control for underwater vehicles. *MDPI Journal of Marine Science Engineering* 8, 4 (2019), 55.
- [107] Takuya Shimura, Yukihiko Kida, and Mitsuyasu Deguchi. 2019. High-rate acoustic communication at the data rate of 69 kbps over the range of 3,600 m developed for vertical uplink communication. In *Proc. MTS/IEEE OCEANS*, Marseille, France.
- [108] Paul C. Etter. 2003. *Underwater Acoustic Modeling and Simulation* (3 ed.). Spon Press, Taylor & Francis Group.
- [109] Bernd-Christian Renner, Jan Heitmann, and Fabian Steinmetz. 2020. AHOI: Inexpensive, low-power communication and localization for underwater sensor networks and AUVs. *ACM Transactions on Sensor Networks* 16, 2 (Jan. 2020).
- [110] FUSION 6G LONG BASELINE POSITIONING (LBL) SYSTEM. ([n. d.]). <https://www.sonardyne.com/products/fusion-2/>. Last time accessed: Feb. 2021.
- [111] SUBSEA MAPPING SYSTEMS. ([n. d.]). <https://www.kongsberg.com/maritime/products/mapping-systems/mapping-systems/>. Last time accessed: Feb. 2021.
- [112] Nortek DVL. ([n. d.]). <https://www.nortekgroup.com/products/subsea-navigation>. Last time accessed: Feb. 2021.
- [113] F. Campagnaro et al. 2017. Multimodal underwater networks: Recent advances and a look ahead. In *Proc. ACM WUWNet*. Halifax, Canada.
- [114] R. Petroccia, G. Zappa, T. Furfaro, J. Alves, and L. D’Amaro. 2018. Development of a software-defined and cognitive communications architecture at CMRE. In *OCEANS 2018 MTS/IEEE Charleston*. 1–10. DOI: <http://dx.doi.org/10.1109/OCEANS.2018.8604849>
- [115] Chhagan Lal, Roberto Petroccia, Mauro Conti, and João Alves. 2016. Secure underwater acoustic networks: Current and future research directions. In *IEEE UComms*.
- [116] M. M. Zuba, Z. Shi, Z. Peng, and J.-H. Cui. 2011. Launching denial-of-service jamming attacks in underwater sensor networks. In *Proceedings of the Sixth ACM International Workshop on Underwater Networks (WUWNet'11)*. Seattle, Washington, USA.
- [117] Lu Ma, Cheng Fan, Wei Sun, and Gang Qiao. 2018. Comparison of jamming methods for underwater acoustic DSSS communication systems. In *IEEE Advanced Information Management, Communicates, Electronic and Automation Control Conference (IMCEC)*.
- [118] Filippo Campagnaro, Davide Tronchin, Alberto Signori, Roberto Petroccia, Konstantinos Pelekanakis, Pietro Paglierani, João Alves, and Michele Zorzi. 2020. Replay-attack countermeasures for underwater acoustic networks. In *Proc. MTS/IEEE Oceans*. Virtual Conference.
- [119] G. Cario, A. Casavola, P. Gjanci, M. Lupia, C. Petrioli, and D. Spaccini. 2017. Long lasting underwater wireless sensors network for water quality monitoring in fish farms. In *OCEANS 2017 - Aberdeen*. 1–6. DOI: <http://dx.doi.org/10.1109/OCEANSE.2017.8084777>

- [120] Water Linked Modem M64. ([n. d.]). <https://waterlinked.com/product/modem-m64/>. Last time accessed: Feb. 2021.
- [121] Trittech Micron Modem - Acoustic Modem. <https://www.tritech.co.uk/product/micron-data-modem>. ([n. d.]). Last time accessed: Feb. 2021.
- [122] Desert Star Systems. 2011. SAM-1 Technical Reference Manual. (Jan. 2011). <https://desertstarsystems.nyc3.digitaloceanspaces.com/Manuals/SAM-1TechnicalReferenceManual.pdf>. Last Time Accessed: Feb. 2021.
- [123] Low cost underwater acoustic modem for Makers of Underwater Things and OEMs! ([n. d.]). <https://dspcommgen2.com/news-flash-low-cost-acoustic-modems-and-transducers-available-for-sale-now>. Last time accessed: Sep. 2021.
- [124] Filippo Campagnaro, Roberto Francescon, Davide Tronchin, and Michele Zorzi. 2018. On the feasibility of video streaming through underwater acoustic links. In *Proc. UComms*, Lerici, Italy.
- [125] Dilukshan Karunatilaka, Fahad Zafar, Vineetha Kalavally, and Rajendran Parthiban. 2015. LED based indoor visible light communications: State of the art. *IEEE Commun. Surv. Tutorials* 17, 3 (2015), 1649–1678.
- [126] Navin Kumar and N. R. Lourenco. 2010. Led-based visible light communication system: A brief survey and investigation. *Journal of Engineering and Applied Sciences* 5 (4 2010), 296–307.
- [127] Parth H. Pathak, Xiaotao Feng, Pengfei Hu, and Prasant Mohapatra. 2015. Visible light communication, networking, and sensing: A survey, potential and challenges. *IEEE Commun. Surv. Tutorials* 17, 4 (2015), 2047–2077.
- [128] T. Komine and M. Nakagawa. 2004. Fundamental analysis for visible-light communication system using LED lights. *IEEE Transactions on Consumer Electronics* 50, 1 (2004), 100–107. DOI: <http://dx.doi.org/10.1109/TCE.2004.1277847>
- [129] Chao Shen, Omar Alkhazragi, Xiaobin Sun, Yujian Guo, Tien Khee Ng, and Boon S. Ooi. 2019. Laser-based visible light communications and underwater wireless optical communications: A device perspective. In *SPIE*. 29–37.
- [130] Giuseppe Schirripa Spagnolo, Lorenzo Cozzella, and Fabio Leccese. 2020. Underwater optical wireless communications: Overview. *Sensors* 20, 8 (2020).
- [131] Basem Shihada, Osama Amin, Christopher Bainbridge, Seifallah Jardak, Omar Alkhazragi, Tien Khee Ng, Boon Ooi, Michael Berumen, and Mohamed-Slim Alouini. 2020. Aqua-Fi: Delivering internet underwater using wireless optical networks. *IEEE Communications Magazine* 58, 5 (2020), 84–89.
- [132] Jaime Lloret, Sandra Sendra, Miguel Ardid, and Joel J. P. C. Rodrigues. 2012. Underwater wireless sensor communications in the 2.4 GHz ISM frequency band. *Sensors* 12, 4 (2012), 4237–4264.
- [133] Andrea Caiti, Ernesto Ciaramella, Giuseppe Conte, Giulio Cossu, Daniele Costa, Simone Grechi, Roger Nuti, David Scaradozzi, and Alessandro Sturmiolo. 2016. OptoCOMM: Introducing a new optical underwater wireless communication modem. In *2016 IEEE Third Underwater Communications and Networking Conference (UComms)*. IEEE, 1–5.
- [134] <https://picryl.com/media/us-navy-diver-3rd-class-ryan-doherty-assigned-to-mobile-diving-salvage-unit-1c420e>. ([n. d.]). Last time accessed: June 2022.
- [135] <https://pixabay.com/illustrations/underwater-water-grass-background-2311701/>. ([n. d.]). Last time accessed: June 2022.
- [136] Hassan Makine Oubei, Changping Li, Ki-Hong Park, Tien Khee Ng, Mohamed-Slim Alouini, and Boon S. Ooi. 2015. 2.3 Gbit/s underwater wireless optical communications using directly modulated 520 nm laser diode. *Optics Express* 23, 16 (2015), 20743–20748.
- [137] Joao Alves, John Potter, Piero Guerrini, Giovanni Zappa, and Kevin LePage. 2014. The LOON in 2014: Test bed description. In *2014 Underwater Communications and Networking (UComms)*. IEEE, 1–4.
- [138] Chiara Petrioli and Roberto Petroccia. 2012. SUNSET: Simulation, emulation and real-life testing of underwater wireless sensor networks. *Proceedings of IEEE UComms 2012* (2012), 12–14.
- [139] Alok Sahu, Debasish Ghose, and P. S. Sastry. 2017. Remotely operated vehicle (ROV) IRIS-SP for underwater inspection tasks. In *2017 14th IEEE India Council International Conference (INDICON)*. IEEE, 1–6.
- [140] Chiara Petrioli, Roberto Petroccia, and Daniele Spaccini. 2013. SUNSET version 2.0: Enhanced framework for simulation, emulation and real-life testing of underwater wireless sensor networks. In *Proceedings of the Eighth ACM International Conference on Underwater Networks and Systems*. 1–8.
- [141] Alberto Signori, Filippo Campagnaro, and Michele Zorzi. 2018. Modeling the performance of optical modems in the DESERT underwater network simulator. In *2018 Fourth Underwater Communications and Networking Conference (UComms)*. IEEE, 1–5.
- [142] Jeffrey H. Smart. 2005. Underwater optical communications systems part 1: Variability of water optical parameters. In *MILCOM 2005-2005 IEEE Military Communications Conference*. IEEE, 1140–1146.
- [143] Riccardo Masiero, Saiful Azad, Federico Favaro, Matteo Petrani, Giovanni Toso, Federico Guerra, Paolo Casari, and Michele Zorzi. 2012. DESERT underwater: An NS-miracle-based framework to design, simulate, emulate and realize test-beds for underwater network protocols. In *2012 OCEANS-Yeosu*. IEEE, 1–10.
- [144] Design, Simulate, Emulate, and Realize Test-beds for Underwater Network Protocols. <https://www.sonardyne.com/bluecomm-whats-what/>. ([n. d.]).
- [145] BlueComm. <https://www.sonardyne.com/bluecomm-whats-what/>. ([n. d.]).

- [146] Marek Doniec, Carrick Detweiler, Iuliu Vasilescu, Mandar Chitre, Matthias Hoffmann-Kuhnt, and Daniela Rus. 2010. AquaOptical: A lightweight device for high-rate long-range underwater point-to-point communication. *Marine Technology Society Journal* 44, 4 (2010), 55–65.
- [147] Marek Doniec, Anqi Xu, and Daniela Rus. 2013. Robust real-time underwater digital video streaming using optical communication. In *2013 IEEE International Conference on Robotics and Automation*. IEEE, 5117–5124.
- [148] Fatah Almabouada, Manuel Adler Abreu, João M. P. Coelho, and Kamal Eddine Aiadi. 2019. Experimental and simulation assessments of underwater light propagation. *Frontiers of Optoelectronics* 12, 4 (2019), 405–412.
- [149] Nils Gunnar Jerlov. 1977. Classification of sea water in terms of quanta irradiance. *ICES Journal of Marine Science* 37, 3 (1977), 281–287.
- [150] YAG laser. https://www.rp-photonics.com/yag_lasers.html. ([n. d.]).
- [151] Ray trace faster using user-defined objects in OpticStudio, Zemax. <https://www.zemax.com/blog/zemax-blog/november-2019/ray-trace-faster-using-user-defined-objects-in-opt>. ([n. d.]).
- [152] BlueComm 100. <https://www.sonardyne.com/product/bluecomm-underwater-optical-communication-system/>. ([n. d.]).
- [153] BlueComm 200. <https://www.sonardyne.com/product/bluecomm-200-wireless-underwater-video/>. ([n. d.]).
- [154] bluecomm200UV-underwater-optical-communication-system. https://www.sonardyne.com/app/uploads/2016/06/Sonardyne_8361_BlueComm_200_UV.pdf. ([n. d.]).
- [155] The OpenSceneGraph Project, OpenSceneGraph. <http://www.openscenegraph.org/>. ([n. d.]).
- [156] Bullet Real-Time Physics Simulation. <https://pybullet.org/wordpress/>. ([n. d.]).
- [157] bulletpysics, Github. <https://github.com/bulletpysics/bullet3.git>. ([n. d.]).
- [158] Diego Centelles, Antonio Soriano, J. Vicente Martí, Raúl Marin, and Pedro J. Sanz. 2019. UWSim-NET: An open-source framework for experimentation in communications for underwater robotics. In *OCEANS 2019-Marseille*. IEEE, 1–8.
- [159] Daniel Cook, Andrew Vardy, and Ron Lewis. 2014. A survey of AUV and robot simulators for multi-vehicle operations. In *2014 IEEE/OES Autonomous Underwater Vehicles (AUV)*. IEEE, 1–8.
- [160] Peng Xie, Zhong Zhou, Zheng Peng, Hai Yan, Tiansi Hu, Jun-Hong Cui, Zhijie Shi, Yunsi Fei, and Shengli Zhou. 2009. Aqua-Sim: An NS-2 based simulator for underwater sensor networks. In *OCEANS 2009*. IEEE, 1–7.
- [161] Gilberto Echeverria, Nicolas Lassabe, Arnaud Degroote, and Séverin Lemaignan. 2011. Modular open robots simulation engine: Morse. In *2011 IEEE International Conference on Robotics and Automation*. IEEE, 46–51.
- [162] Game Engine, Blender Manual. https://docs.blender.org/manual/en/2.79/game_engine/index.html. ([n. d.]).
- [163] Eirik Hexeberg Henriksen, Ingrid Schjølberg, and Tor Berge Gjersvik. 2016. UW MORSE: The underwater modular open robot simulation engine. In *2016 IEEE/OES Autonomous Underwater Vehicles (AUV)*. IEEE, 261–267.
- [164] An Overview of MOOS-IvP and a Users Guide to the IvP Helm - Release 19.8. <https://oceanai.mit.edu/ivpman/pmwiki/pmwiki.php?n=Helm.Cover>. ([n. d.]).
- [165] Gazebo: Robot simulation tool. <http://gazebo.org/>. ([n. d.]).
- [166] Simbody: Multibody Physics API. <https://simtk.org/projects/simbody>. ([n. d.]).
- [167] Thomio Watanabe, Gustavo Neves, Rômulo Cerqueira, Tiago Trocoli, Marco Reis, Sylvain Joyeux, and Jan Albiez. 2015. The rock-gazebo integration and a real-time AUV simulation. In *2015 12th Latin American Robotics Symposium and 2015 3rd Brazilian Symposium on Robotics (LARS-SBR)*. IEEE, 132–138.
- [168] Hydrodynamics, Gazebo Simulation. <http://gazebo.org/tutorials?tut=hydrodynamics&cat=physics>. ([n. d.]).
- [169] Weihua Zhang and David R. Montgomery. 1994. Digital elevation model grid size, landscape representation, and hydrologic simulations. *Water Resources Research* 30, 4 (1994), 1019–1028.
- [170] Musa Morena Marcusso Manhães, Sebastian A. Scherer, Martin Voss, Luiz Ricardo Douat, and Thomas Rauschenbach. 2016. UUV simulator: A gazebo-based package for underwater intervention and multi-robot simulation. In *OCEANS 2016 MTS/IEEE Monterey*. IEEE, 1–8.
- [171] S. M. T. Islam and A. Ashok. 2019. Empirical characterization of vertical channel in underwater visible light communication. In *2019 14th International Conference on Underwater Networks and Systems (WUWNET)*.
- [172] Zhaoquan Zeng, Shu Fu, Huihui Zhang, Yuhan Dong, and Julian Cheng. 2017. A survey of underwater optical wireless communications. *IEEE Communications Surveys & Tutorials* 19, 1 (2017), 204–238. DOI: <http://dx.doi.org/10.1109/COMST.2016.2618841>
- [173] Aidan Fitzpatrick, Ajay Singhvi, and Amin Arbabian. 2020. An airborne sonar system for underwater remote sensing and imaging. *IEEE Access* 8 (2020), 189945–189959. DOI: <http://dx.doi.org/10.1109/ACCESS.2020.3031808>
- [174] Claudio Moriconi, Giacomo Cupertino, Silvello Betti, and Marco Tabacchiera. 2015. Hybrid acoustic/optic communications in underwater swarms. In *OCEANS 2015 - Genova*. 1–9. DOI: <http://dx.doi.org/10.1109/OCEANS-Genova.2015.7271401>
- [175] Mostafa Zaman Chowdhury, Moh Khalid Hasan, Md. Shahjalal, Md. Tanvir Hossan, and Yeong Min Jang. 2020. Optical wireless hybrid networks: Trends, opportunities, challenges, and research directions. *IEEE Communications Surveys & Tutorials* 22, 2 (2020), 930–966.

- [176] Iuliu Vasilescu, Carrick Detweiler, and Daniela Rus. 2007. Aquanodes: An underwater sensor network. In *Proceedings of the Second Workshop on Underwater Networks*. 85–88.
- [177] N. Farr, A. Bowen, J. Ware, C. Pontbriand, and M. Tivey. 2010. An integrated, underwater optical/acoustic communications system. In *OCEANS'10 IEEE Sydney*. IEEE, 1–6.
- [178] N. E. Farr, J. D. Ware, C. T. Pontbriand, and M. A. Tivey. 2013. Demonstration of wireless data harvesting from a subsea node using a “ship of opportunity”. In *2013 OCEANS-San Diego*. IEEE, 1–5.
- [179] Ashish Kumar Sharma, Sadanand Yadav, Sandeep N. Dandu, Vinay Kumar, Joydeep Sengupta, Sanjay B. Dhok, and Sudhir Kumar. 2016. Magnetic induction-based non-conventional media communications: A review. *IEEE Sensors Journal* 17, 4 (2016), 926–940.
- [180] Muhammad Muzzammil, Niaz Ahmed, Gang Qiao, Imran Ullah, and Lei Wan. 2020. Fundamentals and advancements of magnetic-field communication for underwater wireless sensor networks. *IEEE Transactions on Antennas and Propagation* 68, 11 (2020), 7555–7570.
- [181] Steven Kisseleff, Ian F. Akyildiz, and Wolfgang H. Gerstacker. 2018. Survey on advances in magnetic induction-based wireless underground sensor networks. *IEEE Internet of Things Journal* 5, 6 (2018), 4843–4856.
- [182] Amitangshu Pal and Krishna Kant. 2020. NFMI: Near field magnetic induction based communication. *Computer Networks* 181 (2020), 107548.
- [183] Nasir Saeed, Mohamed-Slim Alouini, and Tareq Y. Al-Naffouri. 2019. Toward the internet of underground things: A systematic survey. *IEEE Communications Surveys & Tutorials* 21, 4 (2019), 3443–3466.
- [184] Amitangshu Pal and Krishna Kant. 2019. NFMI: Connectivity for short-range IoT applications. *Computer* 52, 2 (2019), 63–67.
- [185] Honglei Wang, Kun Zheng, Kunde Yang, and Yuanliang Ma. 2014. Electromagnetic field in air produced by a horizontal magnetic dipole immersed in sea: Theoretical analysis and experimental results. *IEEE Transactions on Antennas and Propagation* 62, 9 (2014), 4647–4655.
- [186] R. W. P. King. 1989. Lateral electromagnetic waves from a horizontal antenna for remote sensing in the ocean. *IEEE Transactions on Antennas and Propagation* 37, 10 (1989), 1250–1255.
- [187] Hongzhi Guo, Zhi Sun, and Pu Wang. 2017. Multiple frequency band channel modeling and analysis for magnetic induction communication in practical underwater environments. *IEEE Transactions on Vehicular Technology* 66, 8 (2017), 6619–6632.
- [188] Osama M. Abo-Seida, Samira Tadros Bishay, and Khaled M. El-Morabie. 2006. Far-field radiated from a vertical magnetic dipole in the sea with a rough upper surface. *IEEE Transactions on Geoscience and Remote Sensing* 44, 8 (2006), 2135–2142.
- [189] Hongzhi Guo, Zhi Sun, and Pu Wang. 2021. Joint design of communication, wireless energy transfer, and control for swarm autonomous underwater vehicles. *IEEE Transactions on Vehicular Technology* 70, 2 (2021), 1821–1835.
- [190] Burhan Gulbahar and Ozgur B. Akan. 2012. A communication theoretical modeling and analysis of underwater magneto-inductive wireless channels. *IEEE Transactions on Wireless Communications* 11, 9 (2012), 3326–3334.
- [191] Zhangyu Li, Soham Desai, Vaishnendr D. Sudev, Pu Wang, Jinsong Han, and Zhi Sun. 2020. Underwater cooperative MIMO communications using hybrid acoustic and magnetic induction technique. *Computer Networks* 173 (2020), 107191.
- [192] S. R. Padyath Ravindran, J.-F. Bousquet, and N. Gaoding. 2018. Characterization of a 3D underwater magneto-inductive transmitter coil array. In *OCEANS 2018 MTS/IEEE Charleston*. IEEE, 1–6.
- [193] Maurice Hott and Peter Adam Hoehner. 2020. Underwater communication employing high-sensitive magnetic field detectors. *IEEE Access* 8 (2020), 177385–177394.
- [194] Niaz Ahmed, Andriy Radchenko, David Pommerenke, and Yahong Rosa Zheng. 2018. Design and evaluation of low-cost and energy-efficient magneto-inductive sensor nodes for wireless sensor networks. *IEEE Systems Journal* 13, 2 (2018), 1135–1144.
- [195] Debing Wei, Li Yan, Chenpei Huang, Jie Wang, Jiefu Chen, Miao Pan, and Yuguang Fang. 2020. Dynamic magnetic induction wireless communications for autonomous-underwater-vehicle-assisted underwater IoT. *IEEE Internet of Things Journal* 7, 10 (2020), 9834–9845.
- [196] Ahmed I. Al-Shamma’a, Andrew Shaw, and Saher Saman. 2004. Propagation of electromagnetic waves at MHz frequencies through seawater. *IEEE Transactions on Antennas and Propagation* 52, 11 (2004), 2843–2849.
- [197] Andrew Shaw, A. I. Al-Shamma’a, S. R. Wylie, and D. Toal. 2006. Experimental investigations of electromagnetic wave propagation in seawater. In *2006 European Microwave Conference*. IEEE, 572–575.
- [198] R. Gulati, A. Pal, and K. Kant. 2019. Experimental evaluation of a near-field magnetic induction based communication system. In *IEEE WCNC*.
- [199] RuBee. <http://ru-bee.com/>. ([n. d.]).
- [200] Near-Field Magnetic Induction for Wireless Audio and Data Streaming. <https://www.futureelectronics.com/resources/get-connected/2017-06/future-electronics-near-field-magnetic-induction>. ([n. d.]).

- [201] Vahid Jamali, Diomidis S. Michalopoulos, Murat Uysal, and Robert Schober. 2016. Link allocation for multiuser systems with hybrid RF/FSO backhaul: Delay-limited and delay-tolerant designs. *IEEE Transactions on Wireless Communications* 15, 5 (2016), 3281–3295.
- [202] B. W. Hobson, R. S. McEwen, J. Erickson, T. Hoover, L. McBride, F. Shane, and J. G. Bellingham. 2007. The development and ocean testing of an AUV docking station for a 21" AUV. In *OCEANS*. 1–6.
- [203] Subsea Internet of Things. <https://d26pw6xcesd4up.cloudfront.net/1433418876/wfs.pdf>. ([n. d.]).
- [204] seatooth S200. <https://d3pcsg2wj9izr.cloudfront.net/files/29501/download/352722/2.pdf>. ([n. d.]).
- [205] Seatooth. <https://en.wikipedia.org/wiki/Seatooth>. ([n. d.]).
- [206] S2C R 7/17. <https://evologics.de/acoustic-modem/7-17/r-serie#specs>. ([n. d.]).
- [207] Freelinc. <http://www.freelinc.com/>. ([n. d.]).
- [208] AQUAmodem 500. <https://www.oceanografialitoral.com/sites/default/files/aquamodem500.pdf>. ([n. d.]).
- [209] AQUAmodem 1000. <https://www.oceanografialitoral.com/sites/default/files/aquamodem1000.pdf>. ([n. d.]).
- [210] Acoustic Modems. http://www.teledynmarine.com/Acoustic_Modems?BrandID=2. ([n. d.]).
- [211] Sonardyne BlueComm. <https://www.sonardyne.com/app/uploads/2016/06/BlueComm.pdf>. ([n. d.]).
- [212] AQUAmodem Op2. <https://www.aquatecgroup.com/images/products/AQUAmodemOp2Datasheet.pdf>. ([n. d.]).
- [213] MATS 3G Specifications. http://www.sercel.com/products/Lists/ProductSpecification/Mats3G_specifications_Sercel_EN.pdf. ([n. d.]).
- [214] G. Baiden and Y. Bissiri. 2007. High bandwidth optical networking for underwater untethered telerobotic operation. In *OCEANS 2007*. 1–9.
- [215] S2C R 18/34. <https://evologics.de/acoustic-modem/18-34/r-serie>. ([n. d.]).
- [216] L. Freitag, K. Ball, J. Partan, P. Koski, and S. Singh. 2015. Long range acoustic communications and navigation in the Arctic. In *OCEANS*. 1–5.
- [217] P. J. Beaujean, E. A. Carlson, J. Spruance, and D. Kriel. 2008. HERMES - a high-speed acoustic modem for real-time transmission of uncompressed image and status transmission in port environment and very shallow water. In *OCEANS*. 1–9.
- [218] Gunther Ardelt, Martin Mackenberg, Jan Markmann, Tim Esemann, and Horst Hellbruck. 2016. A flexible and modular platform for development of short-range underwater communication. In *Proc. ACM WUWNet*, Shanghai, China.
- [219] S. I. Inacio, M. R. Pereira, H. M. Santos, L. M. Pessoa, F. B. Teixeira, M. J. Lopes, O. Aboderin, and H. M. Salgado. 2016. Dipole antenna for underwater radio communications. In *Proc. UComms*, Lerici, Italy.
- [220] Jean-Francois Bousquet, Andrew A. Dobbin, and Yibin Wang. 2016. A compact low-power underwater magneto-inductive modem. In *Proc. ACM WUWNet*, Shanghai, China.
- [221] J. J. Sojdehei, P. N. Wrathall, and D. F. Dinn. 2001. Magneto-inductive (MI) communications. In *MTS/IEEE Oceans 2001. An Ocean Odyssey. Conference Proceedings (IEEE Cat. No.01CH37295)*, Honolulu, Hawaii, USA.
- [222] About Penguin Automated Systems. <http://www.penguinasi.com/>. ([n. d.]). Last time accessed: Sep. 2020.
- [223] LUMA. <https://www.hydronea.com/underwater-wireless-communication/>. ([n. d.]). Last time accessed: Sep. 2020.
- [224] Pedro A. Forero, Stephan Lopic, Cherry Wakayama, and Michele Zorzi. 2014. Rollout algorithms for data storage- and energy-aware data retrieval using autonomous underwater vehicles. In *Proc. ACM WUWNet*. Rome, Italy.
- [225] Seongwon Han, Youngtae Noh, Richard Liang, Roy Chen, Yung-Ju Cheng, and Mario Gerla. 2014. Evaluation of underwater optical-acoustic hybrid network. *IEEE China Communications* 11, 5 (May 2014), 1518–1547.
- [226] Filippo Campagnaro, Federico Favaro, Federico Guerra, Violeta Sanjuan Calzado, Michele Zorzi, and Paolo Casari. 2015. Simulation of multimodal optical and acoustic communications in underwater networks. In *Proc. MTS/IEEE OCEANS*, Genova, Italy.
- [227] HYDRONE. <https://www.saipem.com/en/projects/hydrone-njord-field-development>. ([n. d.]). Last time accessed: Feb. 2022.
- [228] EXRAY. <https://www.hydronea.com/exray-wireless-underwater-drone/>. ([n. d.]). Last time accessed: Feb. 2022.
- [229] Filippo Campagnaro, Federico Guerra, Roe Diamant, Paolo Casari, and Michele Zorzi. 2016. Implementation of a multimodal acoustic-optic underwater network protocol stack. In *Proc. MTS/IEEE OCEANS*, Shanghai, China.
- [230] Igor V. Zhilin, Osama M. Bushnaq, Giulia De Masi, Enrico Natalizio, and Ian F. Akyildiz. 2021. A universal multimode (acoustic, magnetic induction, optical, RF) software defined radio architecture for underwater communication. In *Proc. ACM WUWNet*, Shenzhen, China.

Received 27 October 2021; revised 28 March 2022; accepted 5 June 2022